UPPSALA
UNIVERSITET

ELEKTRO-T 22002

Examensarbete 30 hp

11-2021

Detection of voids in welded joints through sonic inspection

Quality control of welded joints in copper canisters for purpose of permanent storage of used nuclear waste

Bakhtiar Afzalan

Civilingenjörsprogrammet i teknisk fysik

UPPSALA
UNIVERSITET

Detection of voids in welded joints through sonic inspection

Bakhtiar Afzalan

Abstract

This thesis was done in cooperation with SKB Clab in Oskarshamn and studies use of sonic waves for detecting voids and irregularities in the weld joints of copper capsules used for long term storage of radioactive waste. Since these could pose material failure and thereby risk radioactive contamination of ground water it is very important to find means of quality control before storage.

During the welding procedure changes occur to the integrity of the material. The homogenous metal – in this case copper – is distorted and voids appear in and around the welded volume. A non-destructive inspection method is needed to make sure that the metal holds for the strains of long term storage. These strains are not completely known at the moment and therefore the goal of this thesis is mainly to add another tool of inspection for future studies.

The tests are done using ultrasonic mapping of the welded volume. This is achieved by sending ultrasonic pulse through test samples – welded copper pieces – and recording its reflection. The recorded signals are gathered in data matrices and processed using several different signal processing methods in search of irregularities and voids. To enhance the understanding of the results a graphical user interface (GUI) is developed that allows users to visualize the results.

The welded pieces, the ultrasonic mapping and its resulting data sets were delivered to this thesis and the scope of the thesis is to develop the GUI and apply known signal processing methods to the data set.

It is shown that the irregularities do appear and that ultrasonic detection and use of the processing method is useful for quality control of the material. Further field studies are needed to identify maximum number, size and perhaps shapes of irregularities that can be within tolerance levels of the storage project.

Teknisk-naturvetenskapliga fakulteten

Uppsala universitet, Utgivningsort Uppsala/Visby

Handledare: Tomas Olofsson Ämnesgranskare: Ping Wu

Examinator: Juan de Santiago

Sammanfattning

I Sverige används sedan mitten på 60-talet kärnkraftsproducerad el. Att driva kärnkraftverk ger restprodukten använd kärnbränsle som är radioaktivt med lång halveringstid. Det åligger Svensk Kärnbränslehantering AB, SKB, att ta hand om avfallen från de svenska kärnkraftverken. Det finns idag ingen överenskommen och beslutad metod för permanent lagring av avfallet utan all använd bränsle förvaras temporärt i ett mellanlager (Clab [1]). SKB har sedan 1970-talet utvecklat metod för att kunna hantera och förvara det använda bränslet på ett säkert sätt under långa tidsrymder. Den metod som valts för slutförvar innebär att bränslet förvaras i kopparkapslar som i sin tur förvaras djupts ner – ca 500 meter – i urberget omgivet av bentonitlera i 100 000 år. En utmaning som rör kapslarna är alltså hur de kan stå emot korrosion och mekanisk påverkan under den tiden. Dessa kapslar tillverkas homogena men kräver att ett lock av koppar sätts fast på kapseln efter placering av använda bränslestavar. Den förslutningsmetod som har testats innebär olika typer av svetsmetoder. Då svetsning samt hantering av kapslarna kan innebära försvagningar i kopparkapseln genom att introducera håligheter eller brott, och det finns ett behov av att kunna verifiera att kapslarna är intakta innan slutförvaring, måste icke förstörande provningsmetoder tas fram för att kontrollera kapslarna. Olika metoder kan vara röntgenbilder eller ultraljudstester av materialet.

I detta examensarbete läggs fokus på den metod som använder ultraljud genom att sända ultraljudspulser in i materialet och fånga dess eko. Detta utförs sedan över hela provets yta och resulterar i stora mängder ultraljudsinformation om ojämnheter i provet. Vid möte med ett hål i materialet fås exempelvis en signalretur som innehåller information om på vilket djup i materialet som hålet befinner sig. Genom att sammanställa all insamlade data och behandla dessa med hjälp av olika digitala filter kan bruset i datamängden minskas vilket leder till bättre definition av ojämnheterna i materialet. För bearbetning av datamängden har en GUI (Graphical User Interface) tagits fram som möjliggör inläsning av datamängden, visualisering av denna samt innehåller ett antal digitala filter för förbättring av bilden. Målet med detta exjobb är att ge berörda ett verktyg för att bedöma ojämnheter och håligheter i materialet för att i förlängningen kunna ta fram en kravspecifikation på hur intakt materialet behöver vara för att stå emot tiden i 100 000 år.

Contents

1 Introduction

1.1 Background

The Swedish Nuclear Fuel and Waste Management Company (Svensk Kärnbränslehantering Aktiebolag in Swedish, abbreviated SKB) is a company whose primary operations are to manage and dispose nuclear waste and used nuclear fuel [1].

For the purpose of long-term waste storage, copper canisters are to be used. A canister is built so that the lid of the canister is welded on the canister to ensure that no leakage will occur. This weld area is the main source of concern regarding leakage in the copper canisters. Since the welding changes the material structure it can give rise to defected areas called defects such as voids and cracks which possibly develop in size gradually with time and become large so as to cause leakage. Therefore, there is a need of methods to inspect the welds in non-destructive manner and guarantee that there are no defects in the weld area.

Ultrasonic testing is one of the non-destructive techniques that are often used to inspect material in the non-destructive manner. It is well suited for the inspecting of the welds of copper canisters. In cooperation with SKB, Signals and Systems group at Uppsala University obtained an ultrasonic array system to inspect the welds of copper canisters and detect possible defects in them. This system has an array of linearly aligned ultrasonic sensors so that it can inspect a weld area by scanning an ultrasonic beam across the area and display the area in a two dimensional (2D) image in real time. The system has an US-Toolbox intended for containing a number of common signal processing methods as well as various visualisation techniques of the data. To apply different

1.2 Purpose and goals

This master thesis project aims to design a graphical user interface (GUI) for the US-Toolbox to easily interpret images in different colour and scale representations, implement new signal

processing methods, evaluate the results of the processing methods, and display original images and processed image within the same window for comparison.

1.3 Tasks and scope

The procedure of ultrasonic inspection includes gathering ultrasonic data, processing the data and finally evaluating the results. The scope of this thesis is to develop a toolbox for processing and visualising delivered ultrasonic data. The processing stage applies different types of digital filters on gathered data in order to enhance, for example, the signal to noise ratio. The aim of the evaluation process is then to reveal enough information about the test object so that the operator can make a decision regarding the structure of the test object (i.e. if any unacceptable defects can be found).

1.4 Outline of Thesis

This report begins with an introduction to the field of ultrasonic material inspection used for detecting defects within materials, section 2.1. The problems faced by the operators, such as presence of noise in the data, are discussed in section 2.4. The solutions to these problems, those used within this thesis, are presented in sections 2.6 through 2.9. These sections begin with an introduction to the basics of signal processing (2.6) and continue with the description of three noise regression algorithms and a temporal resolution enhancement method used within this thesis. This is followed by the description of the program, Chapter 3, including requirements for the input data and an overview of the graphical methods handed to the user. In order to better enclose the welded area two methods of line tracking, called Adaptive and Polynomial fit, have been included. These methods are explained in section 3.2.4. In order to better understand and also as a verification of the Toolbox a special section has been dedicated to the evaluation of the Toolbox, Chapter 4. Finally, the test object is described in Appendix A followed by the User's Manual for the US-Toolbox in Appendix B.

2 Theory

2.1 Ultrasonic Non-Destructive Evaluation

Ultrasonic non-destructive evaluation (NDE) consists of transmitting ultrasonic waves into the test object and evaluating the backscattered response. The ultrasonic waves going into the object are governed by the laws of wave propagation including reflection and refraction at surfaces between two different materials. The reflection and refraction effects produce the information about the inspected specimen in the received signal. The response may contain, for example, information regarding structure of the material, possible shape and location of defects within the object.

The use of elastic waves in the evaluation of materials is a complex problem. Different wave-types take different shapes and paths. The bulk waves propagate through the material while the surface waves are constrained to the boundaries of the object. Furthermore, the bulk waves have two modes, pressure (longitudinal) waves and shear (transversal) waves. For these waves both the particle displacements and the sound speed are different. Moreover, mode conversions will occur at boundaries giving rise to several wave types, even when the transducer generated only a single wave type.

The identification of defect responses in the ultrasonic signal is the main objective of ultrasonic evaluation. As the waves may both be reflected and refracted, the signal will – disregarding the noise – consist of peaks corresponding to the reflections at different inhomogeneous surfaces. These surfaces can either be irregularities, i.e., holes or simply be the bottom, sides or the top of the test object. The amplitude of the peak is partly connected to the size of the reflecting surface. A small hole or crack will reflect little and instead refract most of the pulse, while a distinct border between two different materials will reflect more of the pulse leading to higher amplitude in the signal response. Since the speed of waves in the test object is known the location of the peaks on the time axis simply becomes a measure of distance to the irregularity that gave rise to the peak in question. Figure 2.1 illustrates this principle.

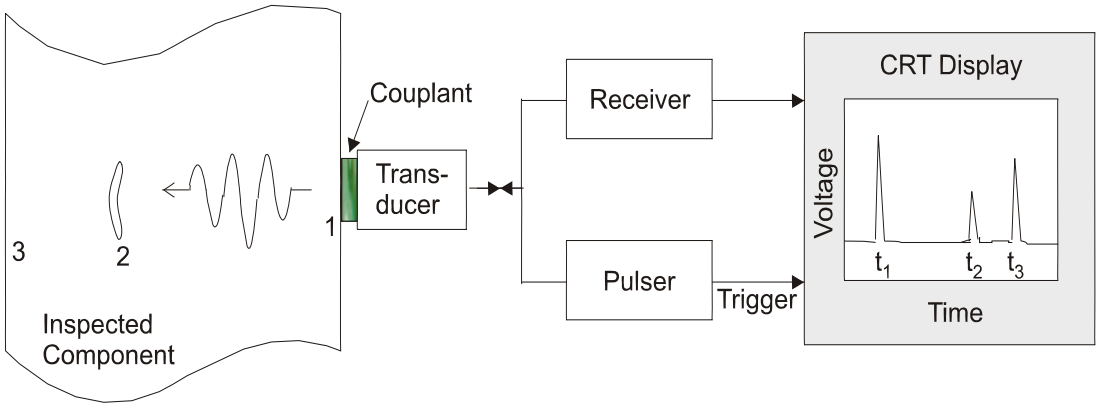

Fig. 2.1 Measurement setup for ultrasonic testing of a specimen. The ultrasonic data consists of a set of signals backscattered at different boundaries within the test-object.

2.2 Ultrasonic Array System

The conversion of an electric pulse into elastic waves can be achieved using a variety of transducer types. Figure 2.2 shows the system used at Signals and Systems group at Uppsala University that is used for gathering ultrasonic data used throughout this report [10].

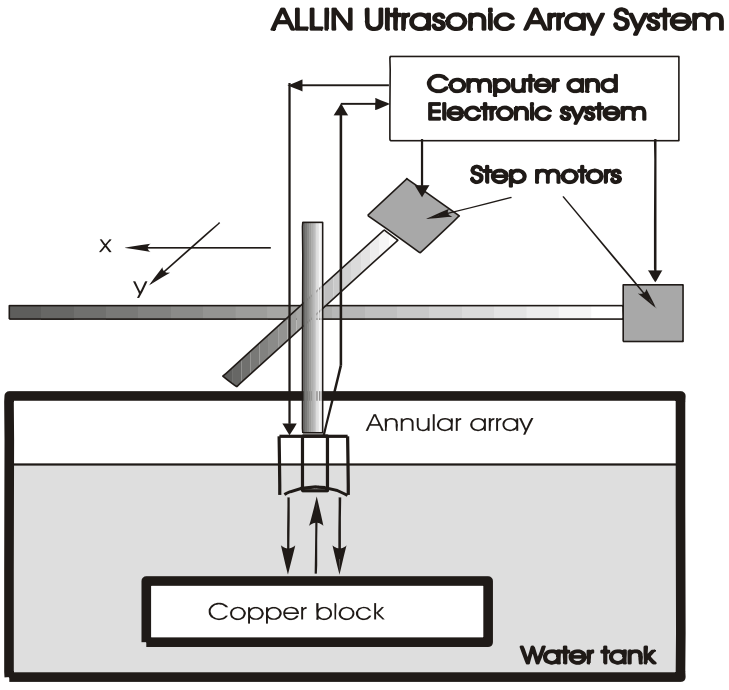

Fig. 2.2 Schematic view of the ALLIN system – setup – used for the measurements at Signals and Systems group.

The most commonly used transducer[1] is the piezoelectric transducer that usually requires some form of couplet connecting it to the object being tested. The couplant can be either water, as is the case in Figure 2.2 – called immersion technique – or a thin layer of gel – called contact technique (water can also be used in the contact method).

Most modern piezoelectric materials are ceramics. The thin disk is the most common shape of piezoelectric ceramics used for non-destructive testing applications. An electric field is applied to the disk causing a change in the thickness of the disk that is proportional to the intensity of the field that lay upon the disk. Depending on the polarity of the electric field, the disk can either contract or expand. The opposite of this energy conversion, i.e. converting mechanical pulses into an electrical signal can also be done using the piezoelectric transducer. This means that a single transducer can be used as both the source of the pulse and the receiver of the backscattered signal, this use of the transducer is called pulse-echo mode.

2.3 Grain Noise

There are means for reducing the noise, for example, by refining the equipment used, or more precisely, the transducer used. The ultrasonic data gathered using one single transducer includes grain noise that depends on the path taken by the ultrasonic beam through the test object. If it is possible to focus the ultrasonic beam on a single point from several different positions and use the average of all those signals as output it will most certainly lead to better resolution in that point. Another way of collecting multiple data from one point is to use array systems. A linear array is a series of transducers connected in a line; this system is shown in Figure 2.3

[1] Another type of transducer is the electromagnetic acoustic transducer, which produces the ultrasonic waves by inducing eddy currents into the object while exposing it to a magnetic field.

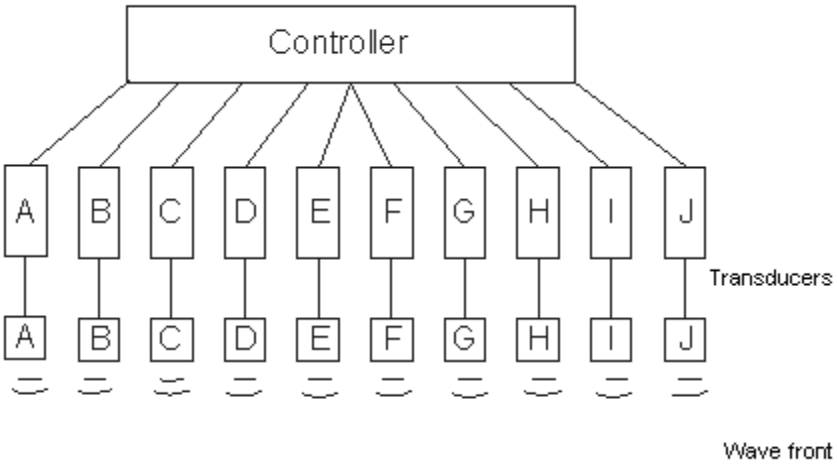

Fig. 2.3 Schematic view of a linear array. A series of transducers are connected to a controller to build an array.

The elements are controlled electronically to allow for beam focusing. The focusing is achieved by introducing different delays to different transducers in the array. The superposition of the pulses from the different transducers will then generate a wave with the direction controlled by the delays. Figure 2.3 presents a simple scheme of a linear array having 10 elements. Common array sizes are 16, 32 or 64 elements.

There are advantages in using an array system compared to a single transducer. Scanning an area with a single transducer requires the use of a mechanical device that controls the position of the transducer. Since ultrasonic inspection sometimes requires very fine resolutions it is necessary to keep two points of measurement as close to each other as possible. This leads to time being consumed simply moving the transducer to the next measurement spot. Using an array the scanning can be performed electronically[2] leading to less time being consumed by data acquisition. That is why ultrasonic evaluation applications are today often performed using arrays instead of single transducers.

To further improve the SNR signal-processing methods can be applied to the acquired ultrasonic data. These methods include digital filters used to suppress the noise. The general idea of all signal-processing methods used for noise reduction is that the signal corresponding

[2] Scanning is achieved by changing the active elements in the array.

to a defect has a distinct pattern while the noise spectrum does not. The signal-processing methods will be discussed more thoroughly in Chapter 3.

Welds and the grain structure of the inspected material give rise to a more complicated problem than one may first expect. An important factor limiting the quality of tests is noise. Here – ultrasonic inspection – a primary source[3] of this noise is called grain noise and is the result of the pulses backscattered at grain boundaries. Figure 2.4 presents the transmitted signal and the corresponding backscattered signal that has been distorted due to the structure of the material.[4]

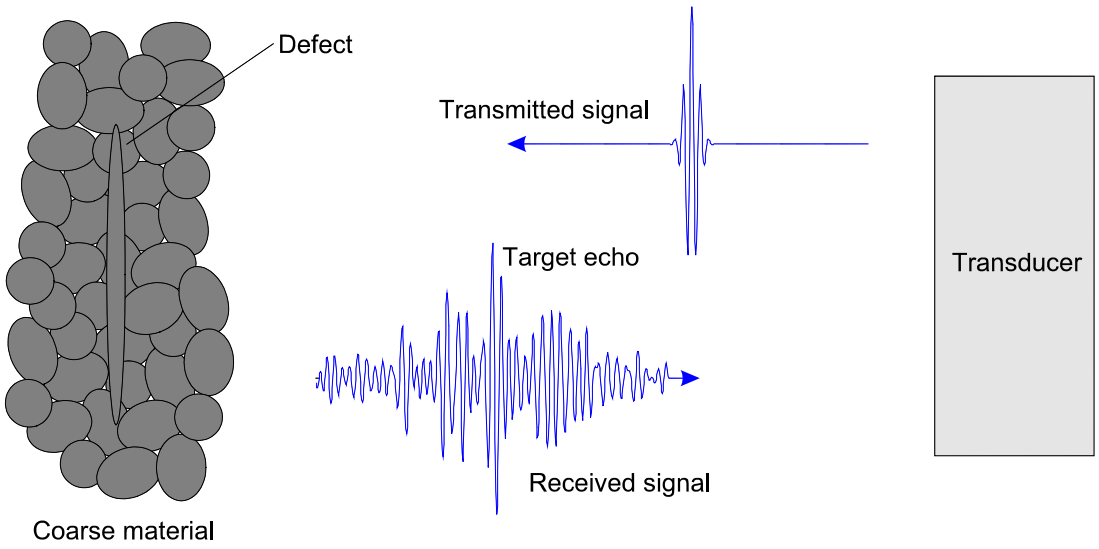

Fig. 2.4 The distortion of the transmitted signal due to grain structure.

2.4 Visualization of Ultrasonic Data

The acquired US-data are stored in vectors containing received signals from the different positions of the transducer. These A-scan vectors can be presented in different forms. The basic approach is plotting the amplitudes as a function of either time or distance. An example of such presentation is shown in Figure 2.5.

[3] There are two sources of noise, measurement noise and the grain noise.
[4] The gathered ultrasonic data will need to be processed in order to repress the noise resulting from both grain and weld structures.

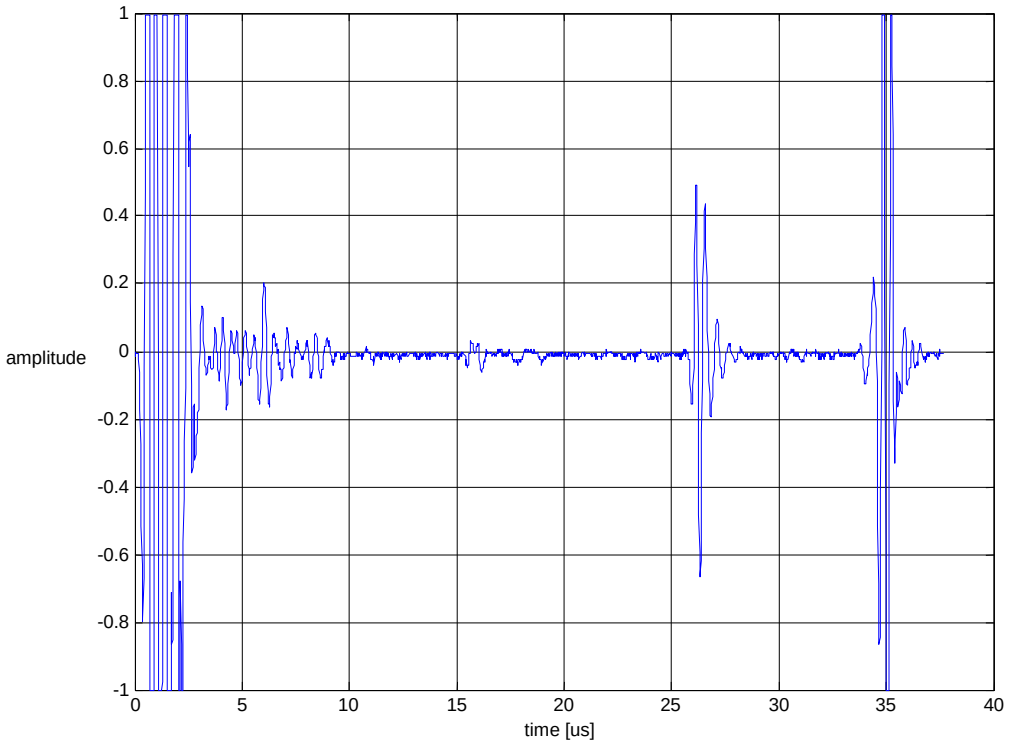

Fig. 2.5 Example of an A-scan taken from a copper specimen. The first echo is the result of the reflection at the front of the specimen and the echo at the end is the result of reflections at the back. The echo observed in between the front and rear reflection represents a hole within the copper specimen.

The peaks in the A-scan in Figure 2.5 indicate the front echo, the back echo or echoes coming from defects within the test object. The information available in an A-scan corresponds to a single measurement. In order to enhance the visual effects, several A-scans taken from different position are put together in one plot to form so-called B-scan. The B-scan represents a two-dimensional surface within the test-object. Then, each horizontal line in the B-scan represents an A-scan with the peaks in the A-scans coded as light or dark areas, depending on the imaging method. An example of a B-scan taken from the CAN1 test block is shown in Figure 2.6 (the CAN1 test block is described in detail in Appendix A). The echo within the marked areas – black rings – in Figure 2.6 originate from side-drilled holes within the test block.

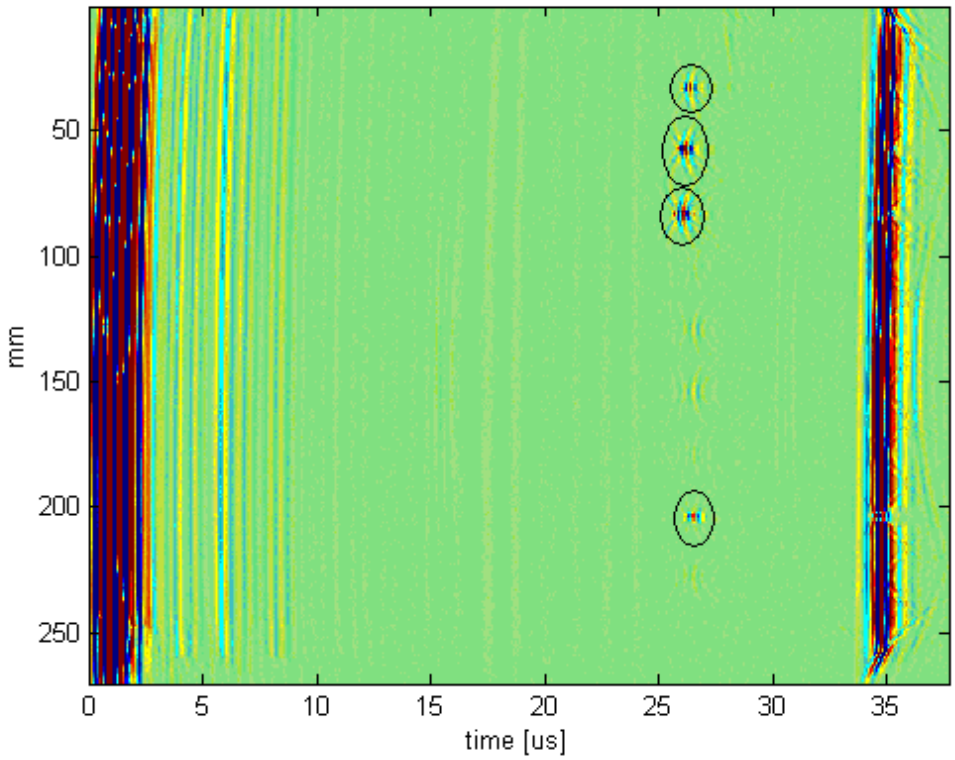

Fig. 2.6 An example of a B-scan taken from the CAN1 test block. The circles mark side drilled holes inside the test object.

Each B-scan covers a vertical slice of the test object. Several B-scan can be taken over the test specimen to cover the entire test object. This results in a three-dimensional US-data covering the entire test-object.

There is a third way of presenting ultrasonic data where the output is the maximum amplitude within a specific time gate. This method is called a C-scan. The C-scan is taken over a set of B-scans within the time gate (or depth). These points are put together to form an image representing flaws at different depths. The image in Figure 2.7 shows an example of a C-scan taken from the CAN1 test-block.

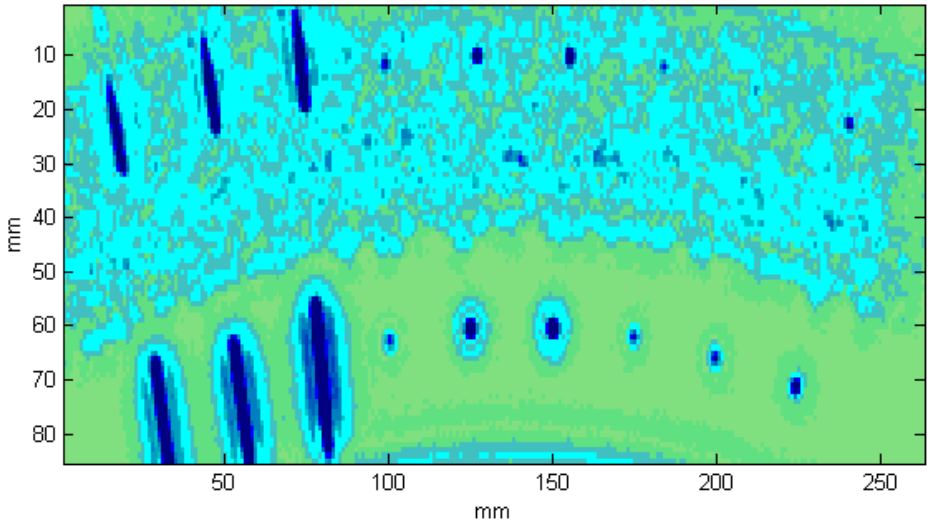

Fig. 2.7 An example of a C-scan taken from the CAN1 specimen. The black areas are flat bottom and side drilled holes within the object. The noisy area is the result of scattering from the weld area.

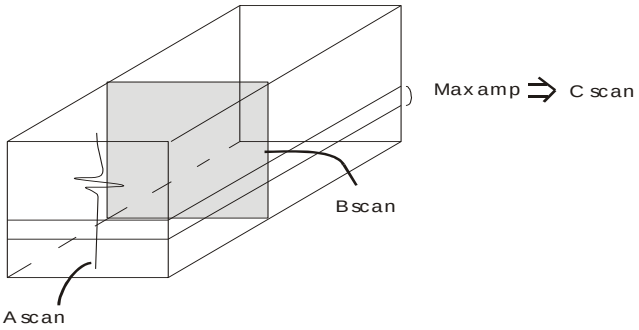

Fig. 2.8 The figure illustrates the data volume and the relation between the different scans.

To facilitate the understanding of the relations between A-, B-, and C-scans Figure 2.8 presents the data volume and the different areas representing the different scan-types. The C-scan extraction operates on a data volume as shown in Figure 2.8.

2.5 Introduction to Signal Processing methods in US-Toolbox

2.5.1 Grain Noise Reduction [7, 8, 9]

This toolbox contains three different methods for grain noise reduction, these are *split spectrum processing (SSP) Minimaization*, *SSP Consecutive Polarity Coincidence* and finally *Common Component Rejection (CCR)*. The common idea among these methods is assuming

different models for the target echo and noise and under those assumptions applying methods to discriminate the noise. Based on the assumption that there are a large number of scatters at random positions within a resolution cell, i.e. the smallest volume that can be resolved, the material noise within an A-scan can be regarded as an interference pattern with maximum and minimum values. The location and amplitude of these extremities depend on the phase differences and intensities of the interfering waves. These quantities depend on the position and the impedances of the reflectors giving rise to the noise pattern. The conclusion is that changing the position of the scatters relative to the inspection beam or changing the size of the scatters relative to the wavelength, i.e. changing inspection frequency, will lead to a change in noise pattern. Two methods of altering the noise pattern are known as the spatial diversity method (SDM) and the frequency diversity method (FDM). The SDM method applies an averaging on signals representing the same point but taken from different positions, while the FDM method applies an averaging in the frequency domain instead. Assuming that defects have a larger cross-section than a single material grain, the FDM and SDM methods can be used to separate between the noise pattern and the target echo pattern.

The SDM is applied when collecting ultrasonic data. Although the FDM could be applied during data collection as well a common way is to use post processing on a single ultrasonic signal (i.e. one A-scan). The idea is to run the signal through a filter bank to simulate the collection of a set of signals using different inspection frequencies. This approach is adopted by the two SSP methods implemented here. The statistical processors available in the toolbox are described in detail in the following sections. The CCR method utilizes a similar assumption as the SSP method, i.e. that noise and target echo spectrums differ. However it makes no assumptions on the spectrum of the target echoes directly but instead estimates the noise spectrum and suppresses the frequencies corresponding to the estimated spectrum. The CCR method is further described in section 2.8.

2.6 Split Spectrum Processing

The SSP methods utilize the FDM approach by splitting a single broadband signal into a set of narrowband signals. Relevant information on defects can then be extracted by processing the split signals using non-linear statistical operations. The first step in the SSP method is called *Expansion* and the second is called *Extraction.* Figure 2.9 illustrates the idea:

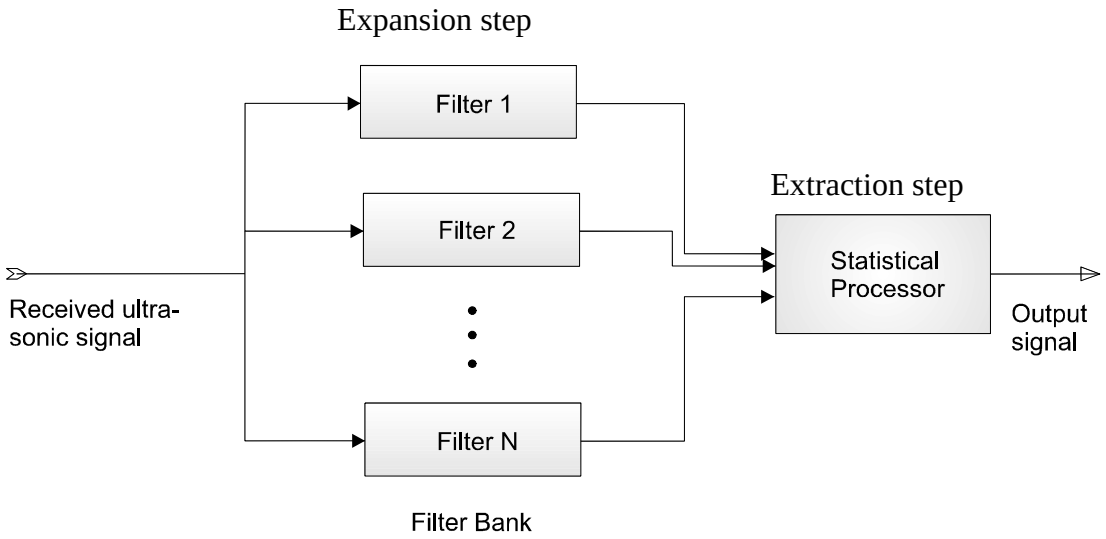

Fig. 2.9 Illustration of the FDM SSP method. The received US-signal is split (expanded) into several frequency bands and processed (extraction) using a statistical processor. The input US-signal, here, is a single A-scan.

2.6.1 The Extraction Process

The set of split signals is now processed using different statistical operations. In this thesis two methods for extraction have been examined[5]. The two methods represent slightly different approach to the problem. These methods are called the Minimization and the Common Polarity Coincidence (CPC) method.

2.6.1.1 Minimization

Following the above discussion regarding the correlation of the noise and the target echo, it is realized that the noise – lacking correlation – can be reduced if the output of the filter is set to the minimum value of the set of signals at each point in time. Since the target echo is highly correlated within the set of signals taking the minimum of the signal would still result in an output greater that the background noise. The algorithm is as follows:

1. For each time instant *kT*, obtain a time-frequency representation of the input signal $s(kT) \Rightarrow \{s_1, s_2, ..., s_n\}$, where $\bar{s} = \{s(1), s(2), ..., s(n)\}$ is the original signal and $s_1, s_2, ..., s_n$ are the split signals resulting from the expansion process.

[5] There are several different methods used for the extraction process, here only the ones mentioned have been included.

2. Find the minimum value at each time instant and set the output to this value i.e.

$y(kT) = \min\{|x_1(kT)|,...,|x_n(kT)|\}$, $y = \{y(1), y(2),..., y(n)\}$ is the output of the process.

Figure 2.11 shows a simulated signal in noisy environment split using two Gaussian windows and the result of the minimization method applied upon these signals.

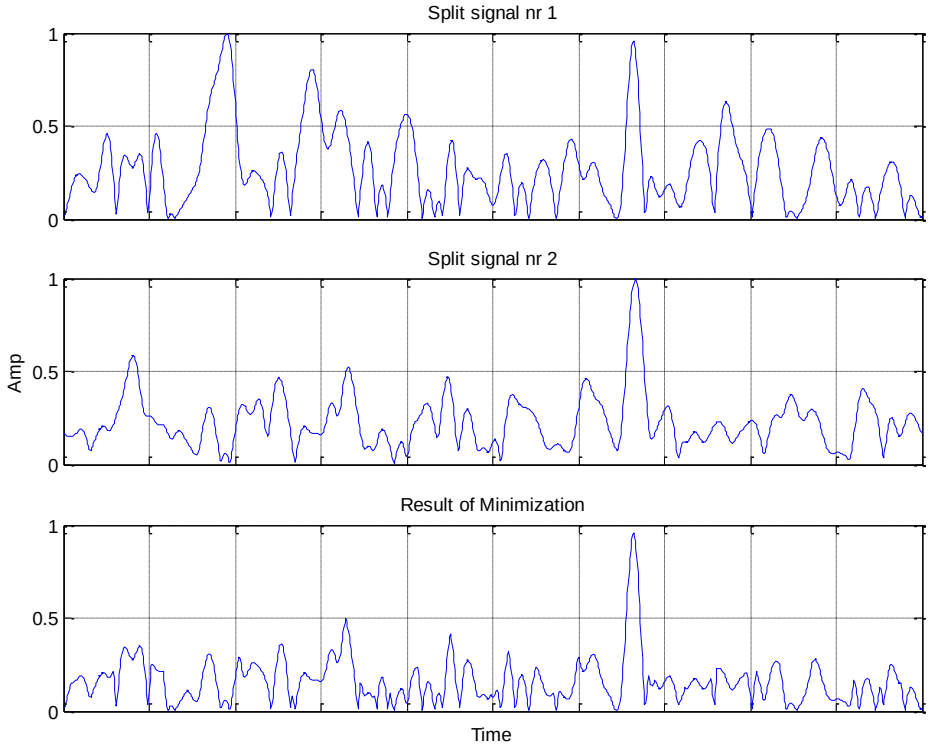

Fig. 2.11 A simulated signal is split into two signals and processed using the Minimization method.

2.6.1.2 Consecutive Polarity Coincidence

The second method, CPC, utilizes the fact that material noise is uncorrelated between the split signals and considers only the polarities of the split signals at each time instant. In the absence of target echo the split signals should reveal an altering sequence of positive and negative amplitudes while the part of the signal containing target echo should have a relatively long sequence of non-altering amplitudes. If the length of the sequence is greater than a specified threshold then the output will be set to the initial input signal, while if the sequence length is smaller than the threshold the output is set to zero. Thus, the method can be summarized in the following steps:

1. For each time instant *kT*, obtain a time-frequency representation of the input signal $s(kT) \Rightarrow \{s_1, s_2, ..., s_n\}$, where $\bar{s} = \{s(1), s(2), ..., s(n)\}$ is the original signal and $s_1, s_2, ..., s_n$ are the split signals resulting from the expansion process.
2. Find the longest sequence $\{s_j, s_j, ..., s_{j+l}\}$ that has the same polarity, i.e. $sign(s_j) = sign(s_{j+1}) = ... = sign(s_{j+l})$, *j = 1, 2, ... , n-l.* $sign(s_j)$ is the sign of the split signal s_j.
3. Set the output *y(kT) = l+1*.
4. The output can be subjected to a threshold to produce the final output, *z(kT)*, from the initial ultrasonic signal *s(kT)* as follows:

$$z(kT) = \begin{cases} s(kT) & y(kT) \geq c \\ 0 & otherwise \end{cases}.$$

2.7 Common Component Rejection

The common component rejection is an algorithm based on a noise model only, which is useful when no reference data is available for calibration. It is based on the assumption that the grain noise is spectrally different from defect responses, more or less statistically stationary and more common than defect indications. By suppressing those frequency components that dominate the response and enhance non-common behavior the noise will be suppressed and hopefully the defects will remain.

This approach, given a noisy area, calculates a spectrum assumed to correspond to the noise. This spectrum is then first normalized and then inversed to give the filter. The result is a band stop filter, repressing those frequencies assumed to correspond to the noise. The resulting filter is:

$$\tilde{P}_n(u) = 1 - \frac{P_n(u)}{|P_n(u)|} \qquad (2.7)$$

where $P_n(u)$ is the power spectrum of the noise process, which is obtained by taking the Fourier transform of the autocorrelation function of the noise. An example of the relation between $P_n(u)$ and $\tilde{P}_n(u)$ is shown in Figure 2.12.

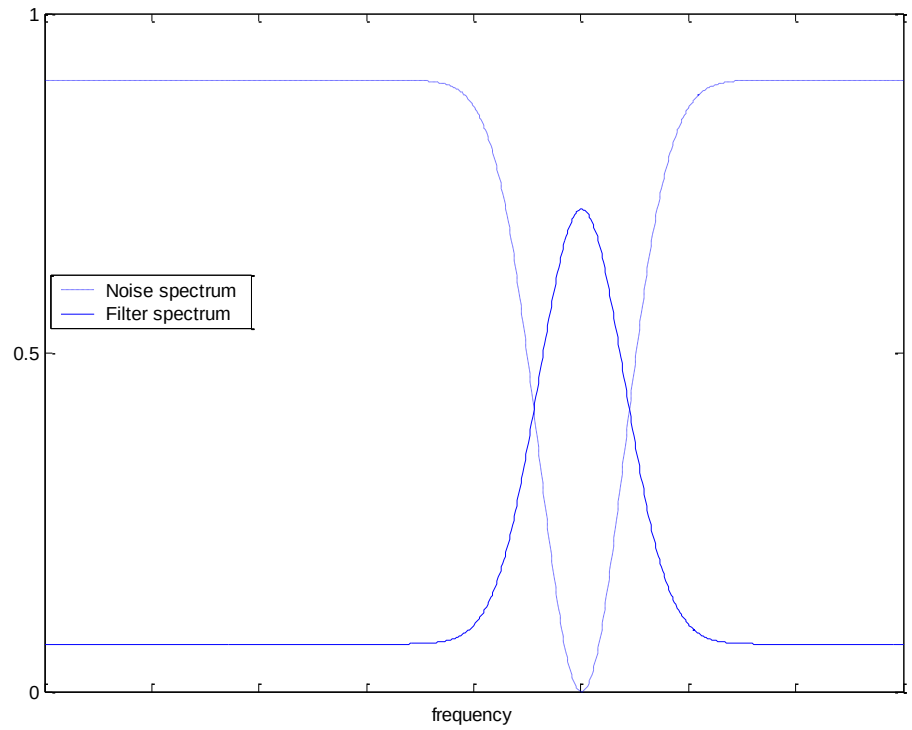

Fig. 2.12 The CCR-filter, dashed line, calculated to suppress the given noise, full line.

Summary Noise Regression

The noise regression methods (CCR, Minimization and CPC) discussed within this chapter give different results on the same data and the choice of filtering method can be difficult. The CCR method, as explained earlier, is very simple and should be used at times when no information is available regarding the spectral properties of the transducer and the target echo. However, do to its simplicity the method doesn't always perform to satisfaction. It should be used with caution and is best suited for quick blind search for defected areas. When spectral information regarding the system is at hand, the operator should generally apply one of the two SSP methods. The difference between the methods is very subtle. The Minimization method can be more reliable since lack of target echo in a single narrowband window can cause the CPC method to perform poorly. However if that does not occur the CPC method generally gives better noise cancellation. Also using the Coherence Threshold (in the CPC method) the operator has a possibility to rule out situations when target echo is missing in a single narrowband window and then use the appropriate method. This argument leads to the conclusion that the CPC method is to prefer when working with the SSP methods, at least it should be the method tested first.

2.8 The Wiener Filter

This method has a different purpose from the methods described above, while the methods described above are mainly noise reducing algorithms, the Wiener filter is a resolution enhancing method, meaning that the focus of the filter in on enhancing the temporal resolution by means of linear filtering. The A-scans are assumed to be degraded by the measuring system. This distortion is due to the systems impulse response. The purpose of the Wiener filter is to estimate the original signal using an approximation of the inverse of the impulse response [6, 11].

Calculation of the Wiener filter requires the assumption that the signal and noise processes are second-order stationary random processes. For this description, only a noise processes with zero mean will be considered (this is without loss of generality) [6, 11].

The Wiener filters used here are applied in the frequency domain. Given a distorted signal *x(u)*, one takes the DFT to obtain *X(u)*. Then the original signal spectrum (i.e. before the signal has been distorted) is estimated by taking the product of *X(u)* with the Wiener filter *G(u):*

$$\hat{S}(u) = G(u)X(u) \tag{2.8}$$

The inverse DFT is then used to obtain the signal estimate from its spectrum. The Wiener filter is defined in terms of these spectra:

$H(u)$	Fourier transform of the system impulse response.
$P_s(u)$	Power spectrum of the signal process $\hat{S}(u)$, obtained by taking the Fourier transform of the signal autocorrelation.
$P_n(u)$	Power spectrum of the noise process, obtained by taking the Fourier transform of the noise autocorrelation.

The Wiener filter is [2]:

$$G(u) = \frac{H^*(u)}{|H(u)|^2 + \frac{P_n(u)}{P_s(u)}} \ . \tag{2.9}$$

The term $\frac{P_n(u)}{P_s(u)}$ can be interpreted as the reciprocal of the signal to noise ratio. Where the signal is very strong relative to noise then $\frac{P_n(u)}{P_s(u)} \approx 0$ and the Wiener filter becomes approximately $H^{-1}(u)$ - the inverse filter for the systems impulse response. If the signal is very weak, $\frac{P_n(u)}{P_s(u)} \to \infty$ and $G(u) \to 0.$ For the case of additive white noise – the case implemented in this toolbox, the Wiener filter simplifies to:

$$G(u) = \frac{H^*(u)}{|H(u)|^2 + \frac{\sigma_n^2}{P_s(u)}} \tag{2.10}$$

where $P_s(u)$ is assumed to be constant so the final filter becomes:

$$G(u) = \frac{H^*(u)}{|H(u)|^2 + \sigma^2} \tag{2.11}$$

where σ^2 is the noise variance. For very high variance values, $\sigma^2 \to \infty,$ the filter becomes

$$G(u) = H^*(u) \tag{2.12}$$

and the output is:

$$\hat{S}(u) = H^*(u)X(u) \tag{2.13}$$

which corresponds to a matched filter resulting in the output being smooth. The other extremity, i.e. $\sigma^2 \to 0,$ gives the following filter:

$$G(u) = \frac{1}{H(u)} \tag{2.14}$$

which is the inverse of the system frequency response. And the output becomes as follows:

$$\hat{S}(u) = H^{-1}(u)X(u). \tag{2.15}$$

Using low variance values gives a noisier output. The result of Wiener filtering using low and high variances is shown in Figures 2.13a and 2.13b. Figure 2.13a shows the unprocessed A-scan:

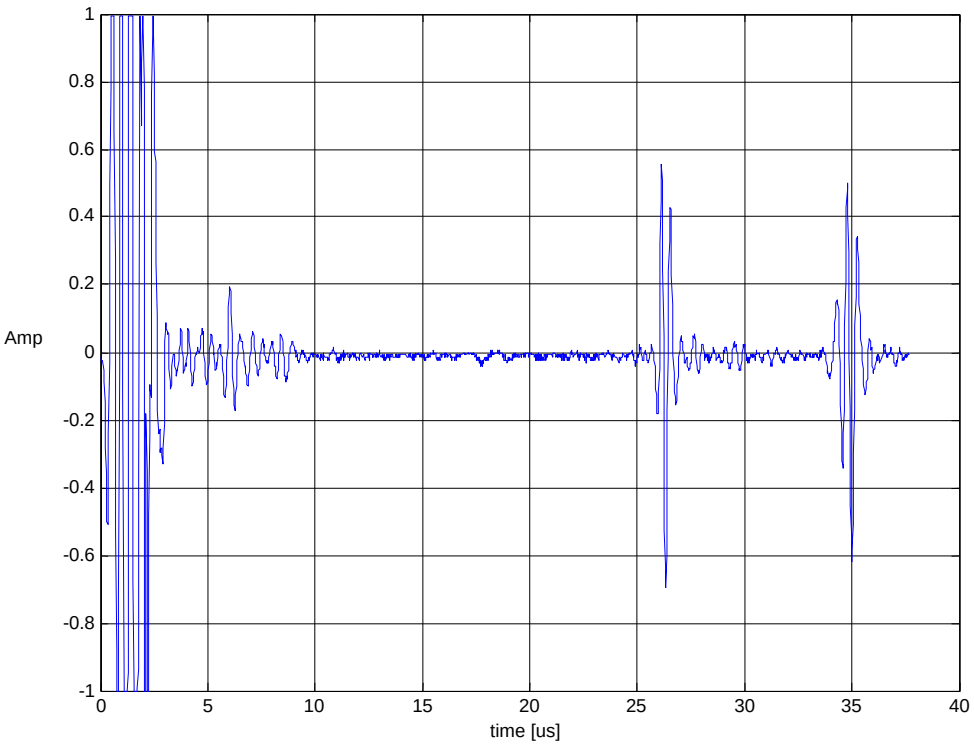

Fig. 2.13a The unprocessed A-scan used for Wiener filtering in the following two Figures.

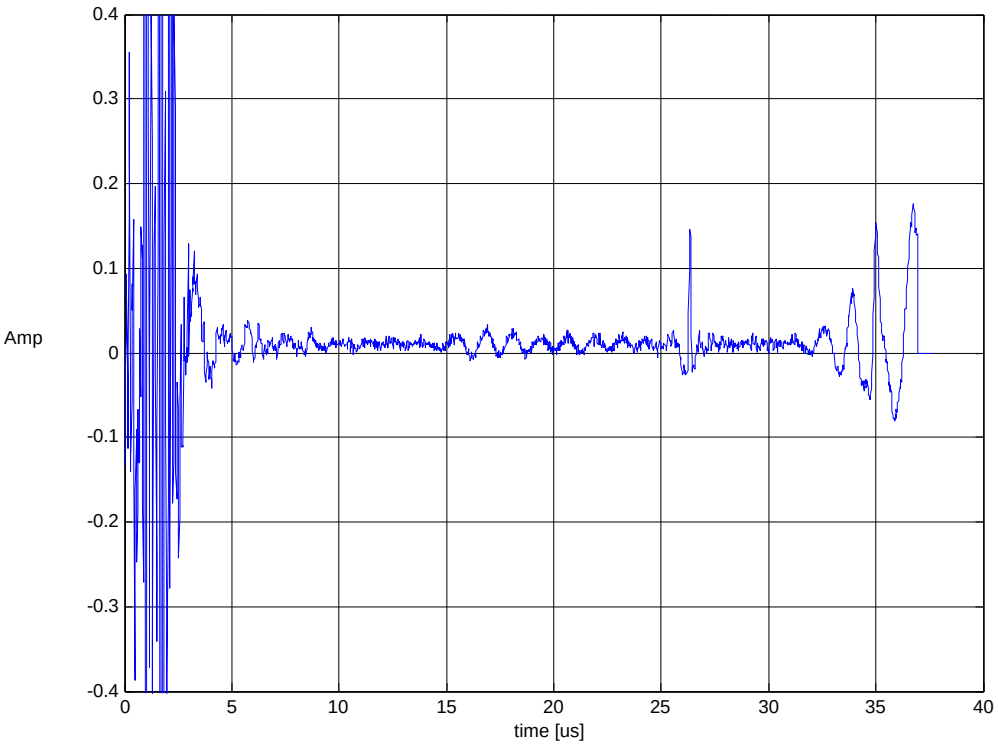

Fig. 2.13b Example of Wiener filtering of the A-scan from Figure 2.13a with σ^2 *set to 0.1.*

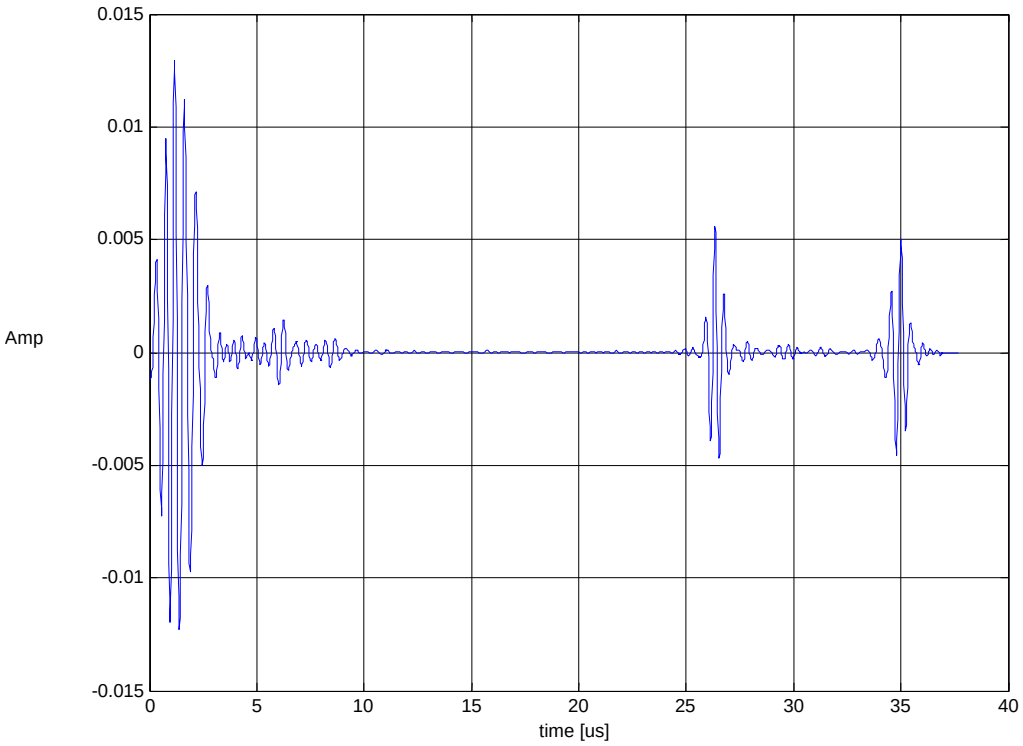

Fig. 2.13c Example of Wiener filtering of the A-scan in Figure 2.13a with σ^2 set to 1000. Note the different y-axis limits in the two Figures.

Figure 2.13b shows the result of filtering the A-scan in Figure 2.13a using the Wiener filter with variance set to 0.1. This Figure clearly illustrates the idea of the Wiener filter, i.e. enhancing the temporal resolution and minimizing the width of the target echoes. The second Figure, 2.13c, shows the result of the Wiener filter applied to the same A-scan but with the variance set to 1000. The difference between the two Figures, 2.13b and 2.13c, is the fact that the former (inverse filter) has a substantial noise included in it while the latter (smoothen filter) seems to be just a smoothening of the original A-scan shown in Figure 2.13a.

3 Ultrasonic image and signal toolbox

3.1 Introduction

This chapter contains a detailed description of the US-Toolbox. Features and examples of using the toolbox will be presented to simplify the understanding of the US-Toolbox. An overview of the structure of the program is also presented.

The main purpose of the US-Toolbox is to process and present the ultrasonic data in an easy interpreted manner. An important part of developing this toolbox has been to keep it user friendly[6]. The program and the graphical user interface (GUI) are both developed using Matlab version 6.1 [3]. A user manual for the GUI can be found in Appendix B.

3.1.1 Guide

The graphical user interface of the US-Toolbox has been developed using the Matlab *Guide* tool [4]. This toolbox can be run under later versions since the functions used will be supported by coming versions. The Matlab G*uide* tool is a graphical tool allowing the user to click and draw in the way similar to common graphic (illustration) programs.

3.2 Graphical user Interface

Typing **ustoolbox** at the command prompt starts the US-Toolbox. The window shown in Figure 3.1 is then opened:

[6] Therefore a graphical user interface (GUI) has been developed.

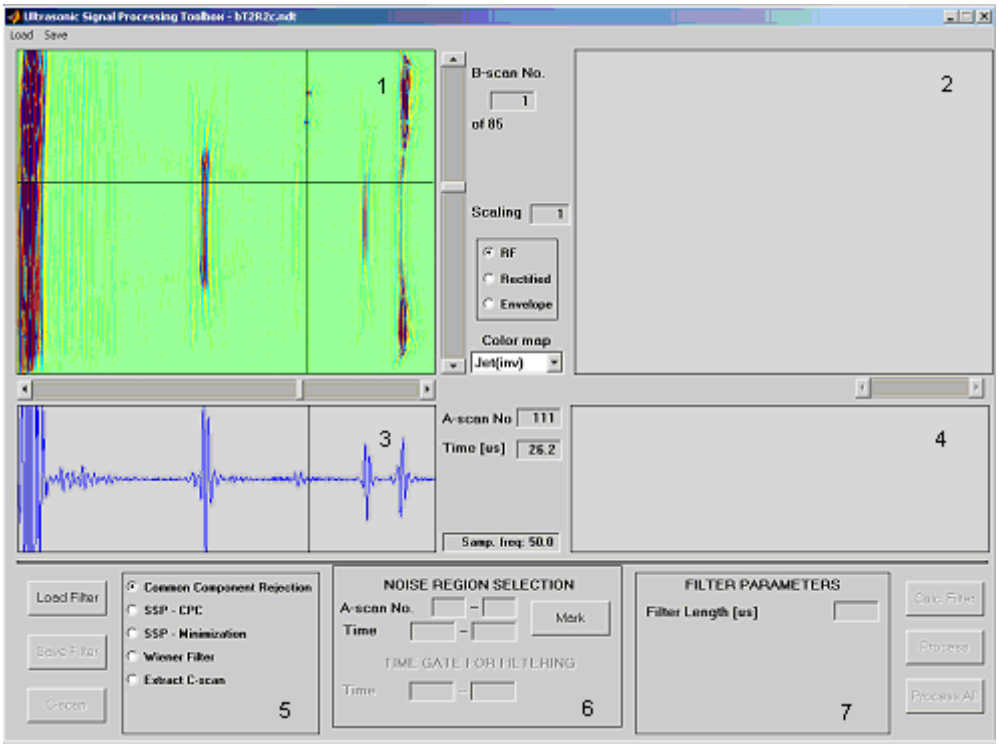

Fig. 3.1 Graphical user interface of the US-Toolbox' main window.

This is the main window containing most of the functions and methods of the toolbox. The window is divided into different areas indicated by numbers in Fig. 3.1. Table 1 presents the function of each part of the main window.

1	Original B-scan window
2	Processed B-scan window
3	Original A-scan window
4	Processed A-scan window
5	Select process field
6	Filter parameters field nr. 1
7	Filter parameters field nr. 2

Table 1. Field numbers in Figure 3.1 and their purpose.

The choice of filter or processing method, in box number 5, controls the properties and presentation of the other two boxes, boxes number 6 and 7. These two in turn include property fields for the different processing methods that need to be defined before processing can occur. There are *Load* and *Save* functions for the filter parameters as well as for B-scan data and C-scan data. The *Save* functions – *Save Filter* or *Save B-scan* – saves the data in the

NDT format **.ndt**. C-scan data however is stored in the native Matlab format **.mat** and is stored using the function *Save C-scan.*

3.3 Load and Save functions

There are three different functions included in the toolbox for loading data, *Load B-scan*, *Load C-scan* and *Radial Load*. The purpose of the first two is to load B-scans or C-scans into the toolbox[7]. The C-scan is then presented in the C-scan window along with the so-called extended C-scan plots (if these where chosen during extraction time). More details on the presentation are found in Chapter 3.2.6 where the Extended C-scan plot is described. The third load option, *Radial Load*, also loads a B-scan into the toolbox. The difference from the normal load function is that *Load B-scan* loads the data as they are acquired, while *Radial Load* loads the data perpendicular to the original acquiring method. When acquiring ultrasonic data the normal procedure is to have the x-axis represent the A-scan numbers, the y-axis represent the B-scan numbers and the z-axis represent the time – see Figure 2.2. The data collected at Signals and Systems follows these rules. Figure 3.2 shows a simplified picture of the CAN1 block used for gathering ultrasonic data and the positions of the two B-scans discussed above.

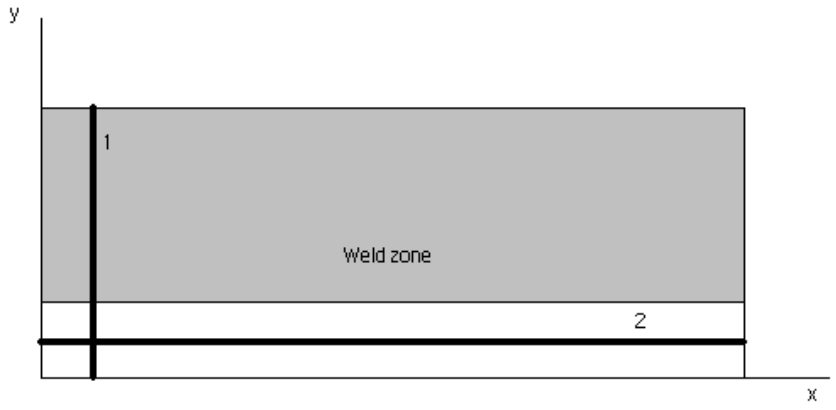

Fig. 3.2 A simplified view of the top of the CAN1 block. Line number 1 represents the direction of the Radial B-scan while line number 2 represents the direction of the original data collection.

The Radial Load loads the data in such an order that the x- and y-axis change place. Now a B-scan is represented by the y- and z-axis instead of x- and z. This method leads to a different

[7] The path and file name of the original data-file giving rise to the C-scan are also stored in this file.

view of the weld area and is suitable to use before applying the *Adaptive* and *Polynomial fit* methods for extracting C-scans, see Section 3.2.6. Examples of the two different data presentation methods are shown in Figure 3.3a and 3.3b respectively:

(a)

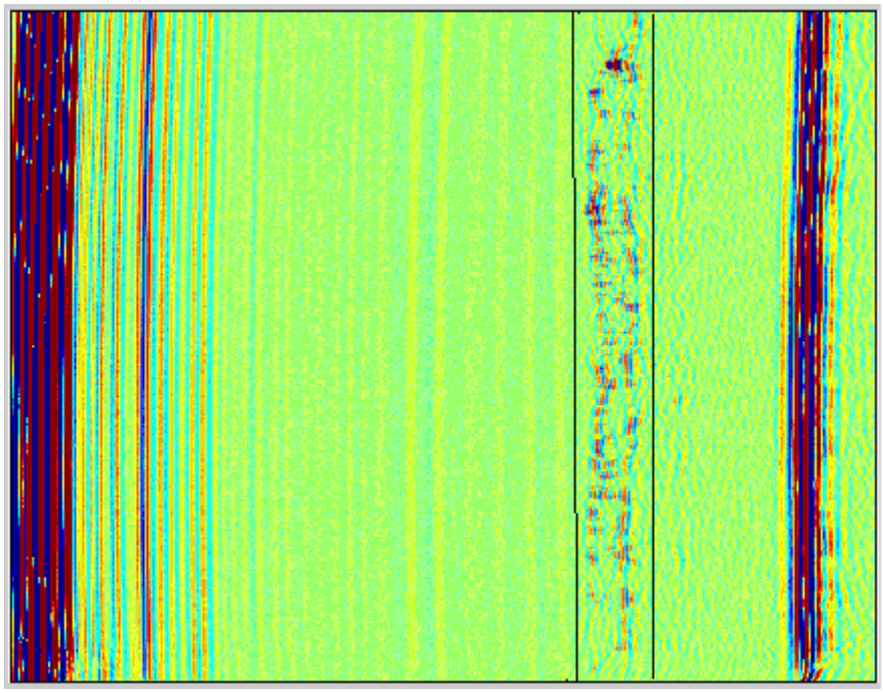

(b)

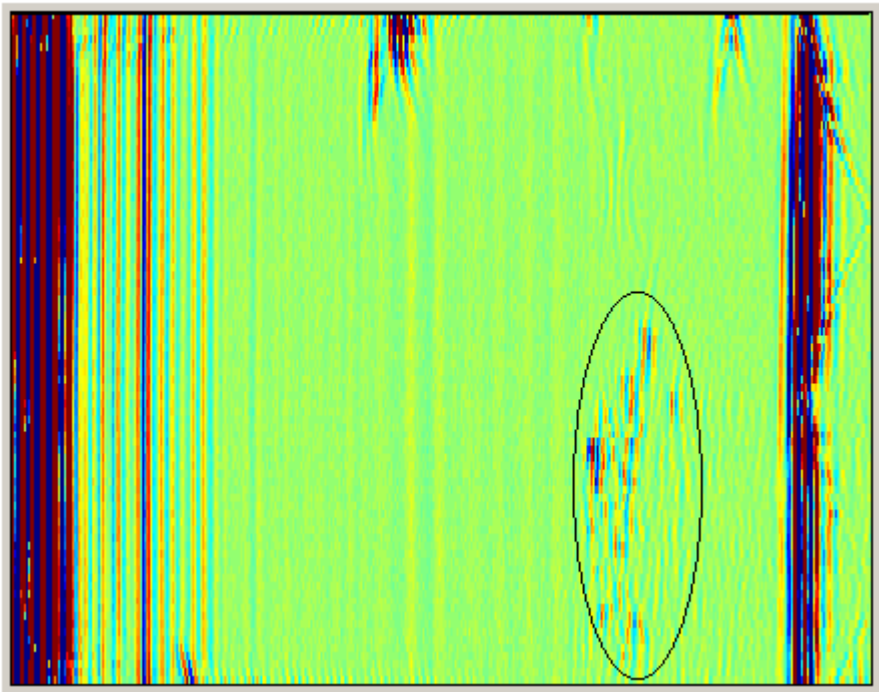

*Fig. 3.3 (a) The Load B-scan method using data from the CAN1 test block. The responses shown in the marked region correspond to the weld, which is well pronounced in the entire B-scan. (b) The **radial** load B-scan method using data from the CAN1 test block. The responses shown in the marked area correspond to the weld. It shows that the cross section of the weld area is different than that in Fig. 3.3 (a).*

3.4 Processing Methods

The program includes several different signal processing methods described in Chapter 2. These methods take different parameters in order to process the ultrasonic data. In the CCR method, the operator is required to choose an area containing noise. The noise autocorrelation function of this area is calculated using the Matlab *xcorr* function and then used to calculate the filter parameters of the CCR, see section 2.8. The parameters used by the SSP methods are:

1. Lower boundary for the frequency.
2. Upper boundary for the frequency.
3. Number of filters.
4. Filter bandwidth.

These values are then applied according to the SSP Expansion theory discussed in section 2.7.1. In addition to the variables above, a fifth variable called Coherence threshold is required by the SSP CPC method. This variable sets a threshold for the output of the CPC method, see section 2.7.4 for details on the CPC method. Examples showing the effect of the filter parameters mentioned above are available in sections 4.3 and 4.4.

The Wiener deconvolution method takes an approximation of the systems frequency response in order to calculate the filter, see section 2.9 for details. This approximation corresponds to ultrasonic measurements from a hole, i.e. the part of an A-scan corresponding to a hole. The quality of this measurement decides the quality of the output of the filter. For information on how to choose this parameter see the manual. Examples showing these different methods at work can be found in Chapter 4.

3.5 Image presentation formats

The program includes a few imaging options. These include different colour-maps, Scaling and finally signal translations. The *Scaling* is simply a constant that is multiplied to the signal to enhance the signal. The *Colour Map* is based on four different colour map functions that are within the Matlab tools. These are called Jet, Jet(inv), Grey and Grey(inv). Choosing

different Colour Maps changes the colours used for presenting the B- or C-scan. Sometimes it is easier to detect irregularities when using one or the other Colour map. Finally there are three different types of interpreting the data, RF, Rectified and Envelope. RF is the presentation of the signal in original form, Rectified is the absolute value of the signal and finally Envelope is the Hilbert transformation of the signal as defined by Matlab, i.e. it calculates the Hilbert transform of the real part of the input signal. The real part of the output represents the original real data where the imaginary part is the actual Hilbert transform. Using different methods can reveal different aspects of the properties of the scans.

3.6 C-scan presentation

Four different presentation methods are implemented in the US-Toolbox for the C-scans.

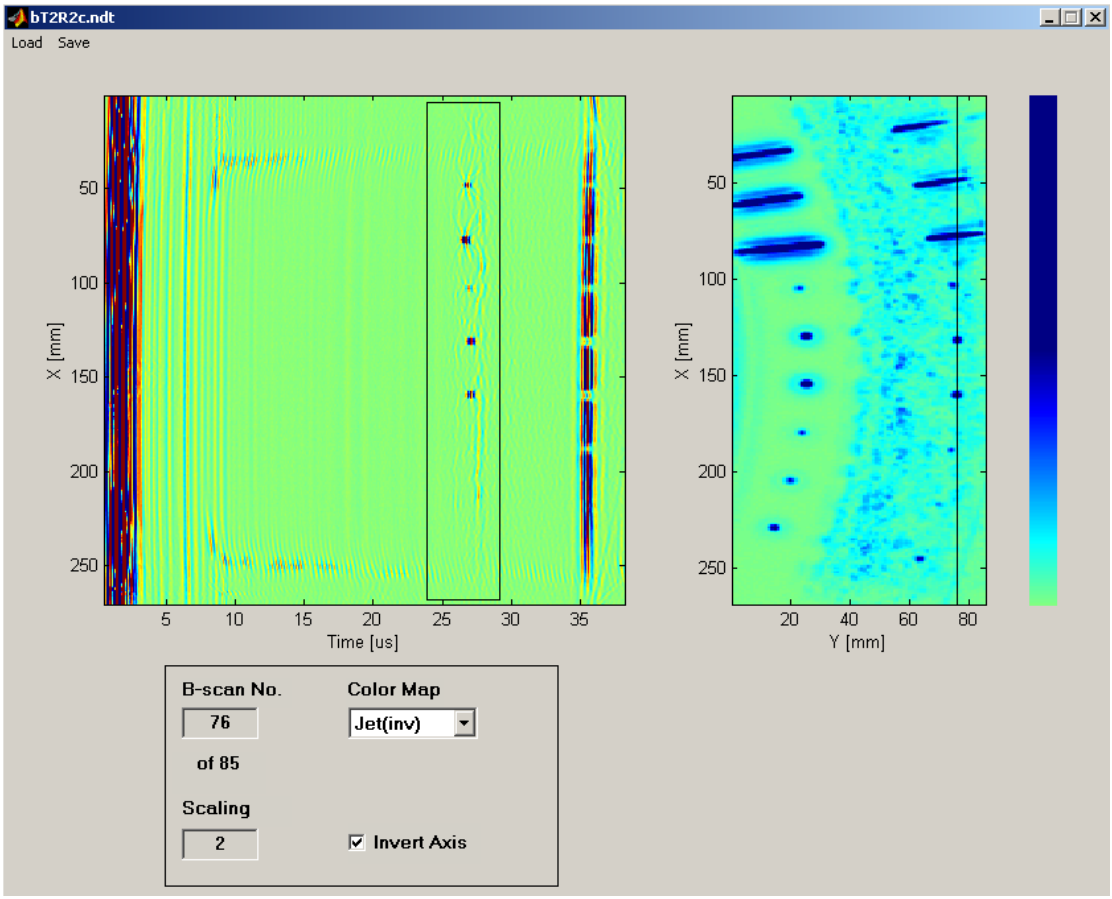

Fig. 3.4 Main window for C-scan presentation.

The C-scan extraction method processes a data cube that consists of a set of B-scans as described in section 2.5. The time-axis and A-scan number-axis boundaries of this data cube are given within a B-scan. The extraction is taking the maximum amplitude within a given time gate in the set of B-scan. The default C-scan extraction method performs the extraction on a rectangular area within each B-scan. The window shown in Figure 3.4 is the main (default) C-scan window used for presenting the C-scans. It includes a C-scan axis – the middle axis, a B-scan axis – the leftmost, and finally a colour order axis that represents different colours and their hierarchical placement towards each other. The B-scan presented in this field corresponds to the black line within the C-scan window.

The choices of different colours and enhancing used for the scans are available also within this window. In addition to the window shown in Figure 3.4 another window has been created for presenting the C-scan in more detail. An example of such a detailed C-scan is presented in Figure 3.5. This window presents the C-scans taken over three different depths within the test-object. This extraction method is optional and is called *Extended C-scan plot.* The result of the extraction is presented in the following window where C-scans are taken over different depths in order to enhance the understanding of the structure within the test-object. The different depths are the results of dividing the extraction area into three parts of equal length. C-scan extraction is then performed on these three depths. The result is richer information on the structure of the object, allowing the user to easier locate the irregularities within the test-object.

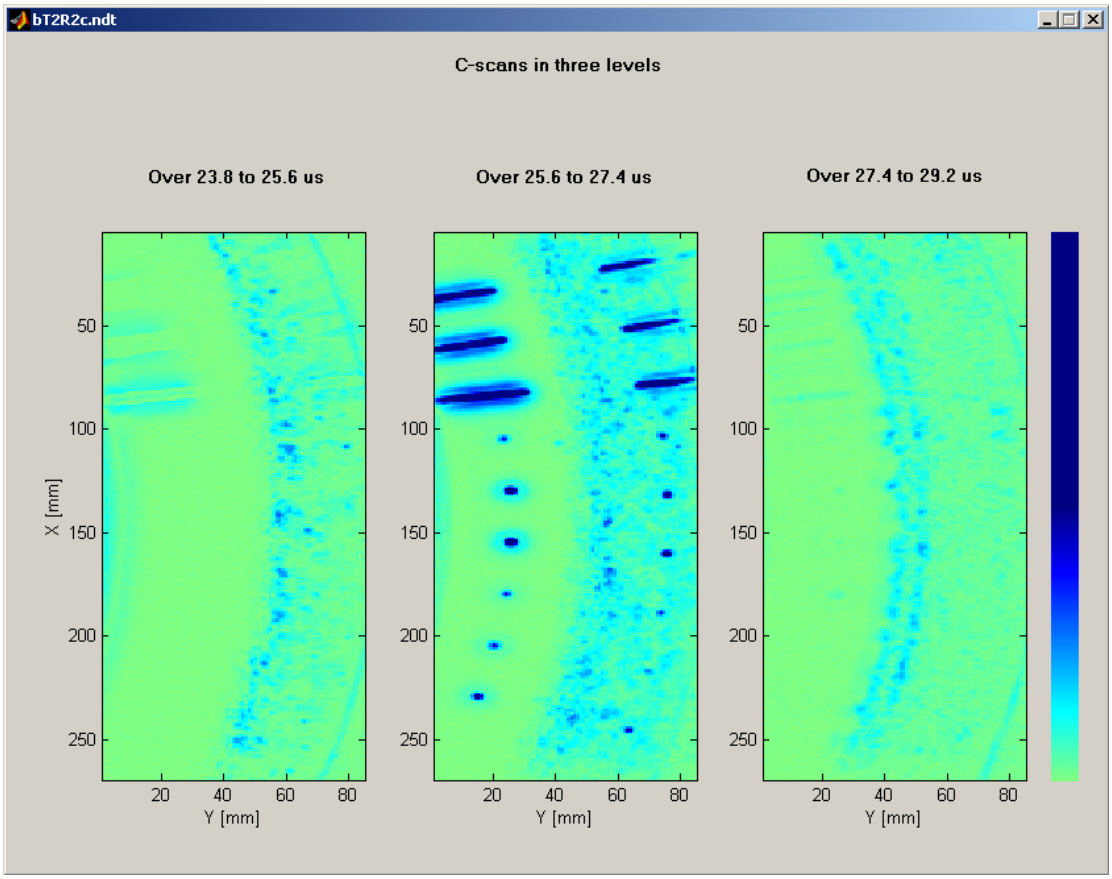

Fig. 3.5 Example of a C-scan extended method used on the CAN1 test block.

3.7 Polynomial fit- and Adaptive Extraction

Since the weld is the part of the canisters that needs extra attention one typically would prefer to concentrate the extraction method to an area consisting of weld only. For this purpose two additional C-scan extraction methods have been developed. The first method called **Polynomial fit** uses the Matlab *spline* function to fit a polynomial to a set of points defined by the user. In order to achieve better result with this method, it is convenient to take the *radial* B-scans instead (Appendix B). The second method of extraction, called **Adaptive,** seeks for the weld surface within an area defined by the user. A Threshold parameter is also passed to this method deciding the sensitivity of the method regarding noise. The weld surface is tracked down using the average of the first 10 time samples of a B-scan (within the given rectangle) and then searching for the first amplitude within an A-scan that is greater than the average times **Threshold**.

In Figure 3.5 the C-scan includes side drilled and flat bottom holes (black areas) but also a welded area including noisy darker shade. This area is the result of the waves backscattered by the weld structure of the CAN1 block. The result of C-scan extraction using the **Polynomial fit** method is shown in Figure 3.6, as in Figure 3.5 above, the area in which the C-scan extraction method is applied is shown in the corresponding B-scan window:

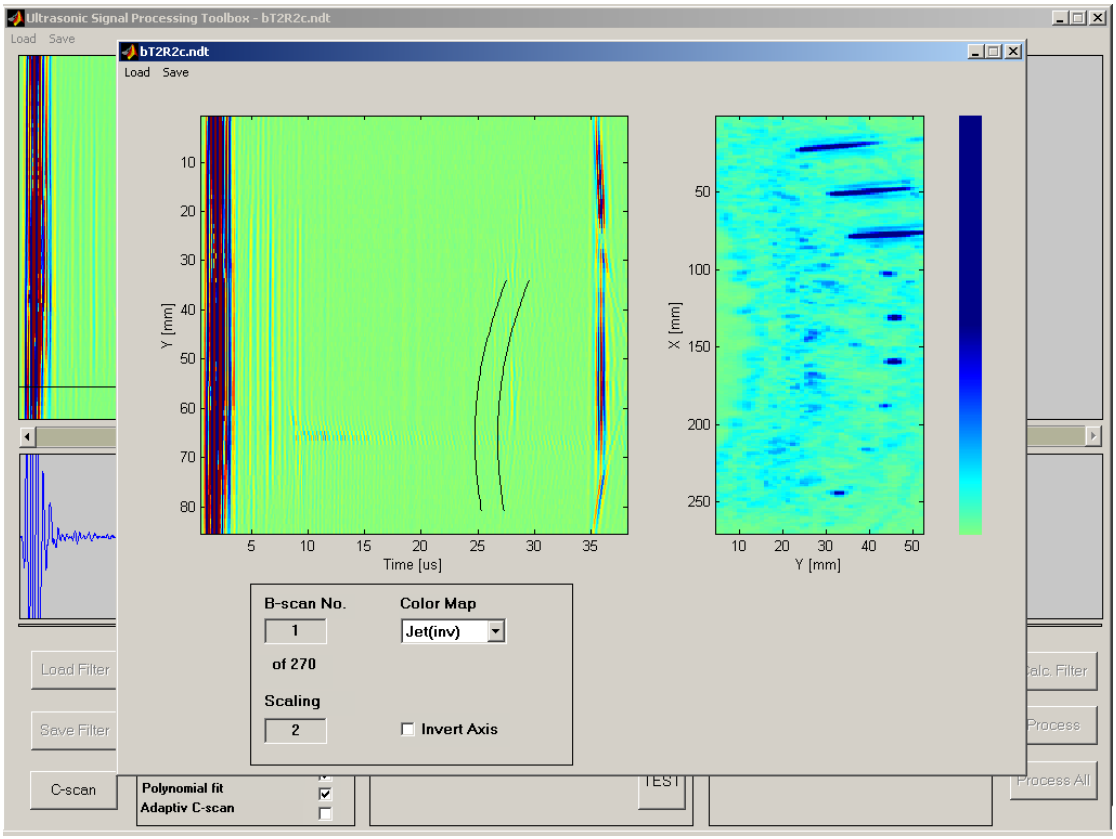

Fig. 3.6 An example of Polynomial fit C-scan taken over a stripe within the B-scan.

The difference between Figure 3.5 and 3.6 is that the former has included signals from areas both outside and inside the weld while the latter contains less intervention from the non-welded areas. Since the extraction method searches for the maximum values over a time interval within each A-scan, strong signals outside the weld could cover important information of the structure within the weld area, such as defects.

In applications where the weld has a border that can better be defined by a straight line it is more convenient to use an alternative of the **Polynomial fit** method. In this method the operator specifies only two points resulting in a straight line instead of a parabolic one used in Figure 3.6.

The third method, **Adaptive** extraction, is presented in Figure 3.7. The advantage of this method is that it can fit the extraction area more closely to the weld area meaning that defects outside the weld are less likely to deteriorate the C-scan.

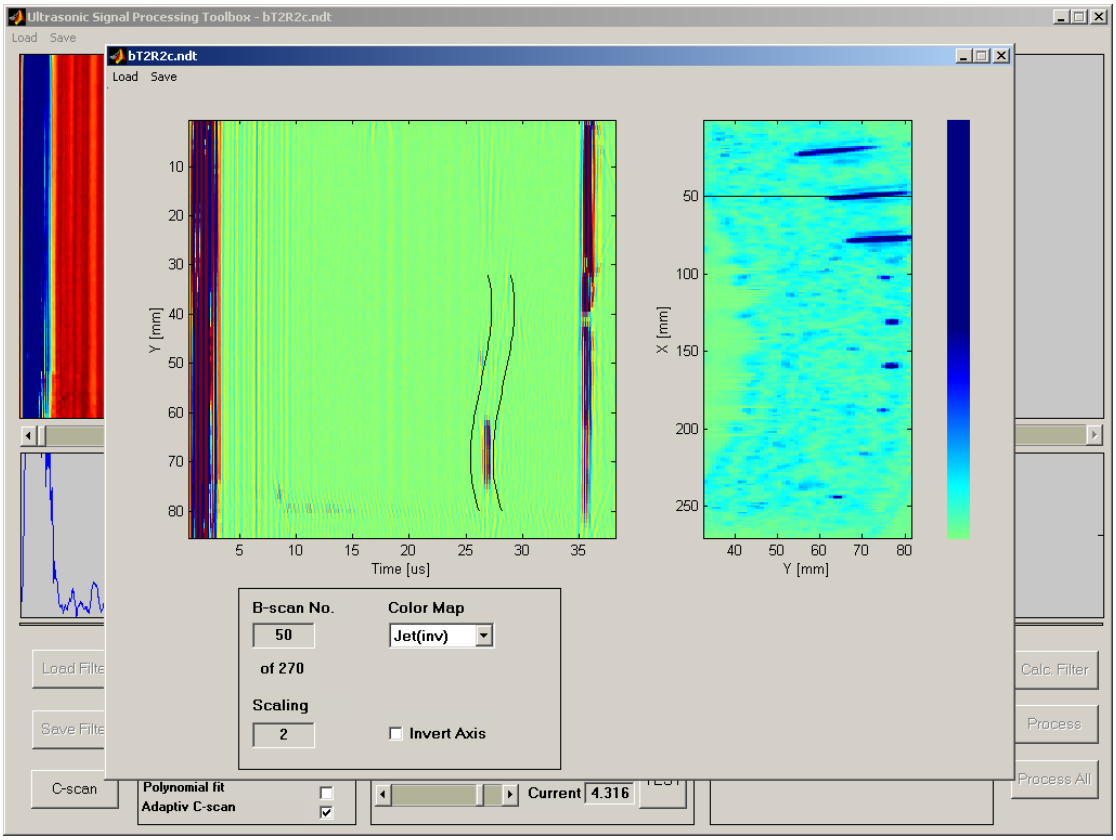

Fig. 3.7 An example of the Adaptive C-scan extraction method used on CAN1. The result is an area that adapts to the weld surface.

By concentrating our maximum amplitude search within this thin stripe, it is less likely that echoes outside the weld zone will cover defects.

4 Evaluation

4.1 Introduction

In this chapter the US-Toolbox is evaluated using data from a copper test specimen CAN1 (see Appendix A). The evaluation will include a thorough examination of some of the more complicated functions, for example functions such as Load or Save will not be evaluated since these functions are of simple nature. Instead, the different processing schemes along with results will be included.

4.2 Common Component Rejection

The purpose of the CCR method is to enhance the signal to noise ratio within the B-scans. Figure 4.1 shows the CCR-filter, calculated for data from the CAN1 block:

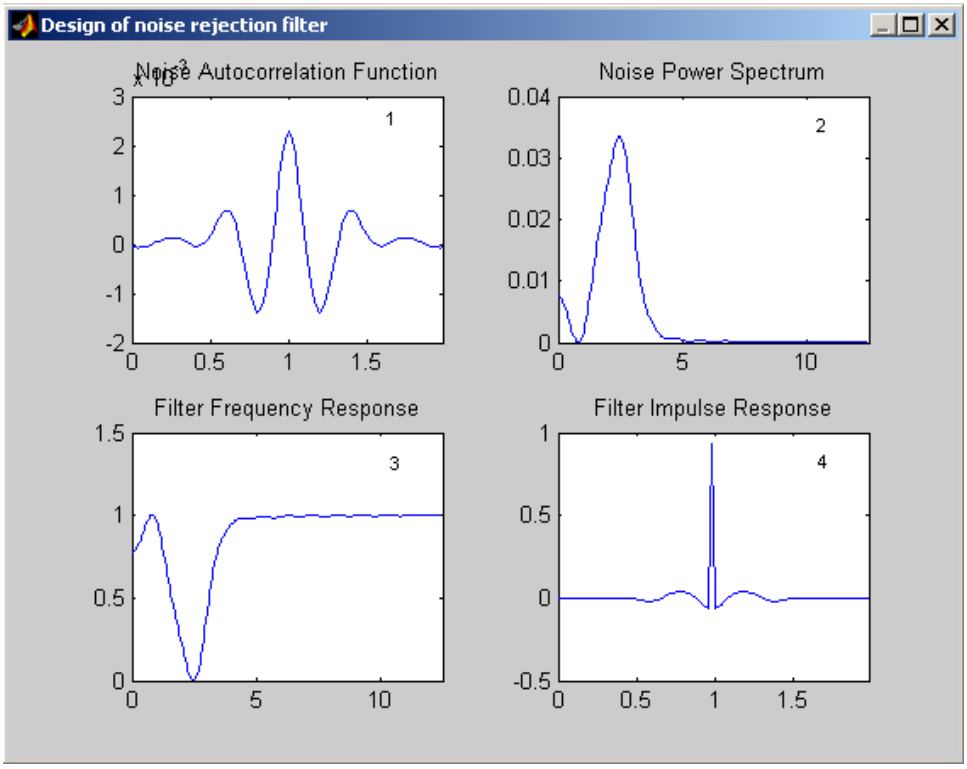

Fig. 4.1 An example of a CCR-filter calculated for the CAN1 block.

The CCR filter is calculated using the noise autocorrelation (box number 1 in Figure 4.1) and noise power spectrum (seen in box 2). A filter is then calculated based on these values. Box 3 in the same figure represents the frequency response of the filter and box 4 contains the corresponding impulse response. The result of the filtering is shown in Figure 4.2. It can be seen from the figure that the filtering process has suppressed the noise but unfortunately it also suppresses the signal resulting in no actual enhancement in the signal to noise ratio (here).

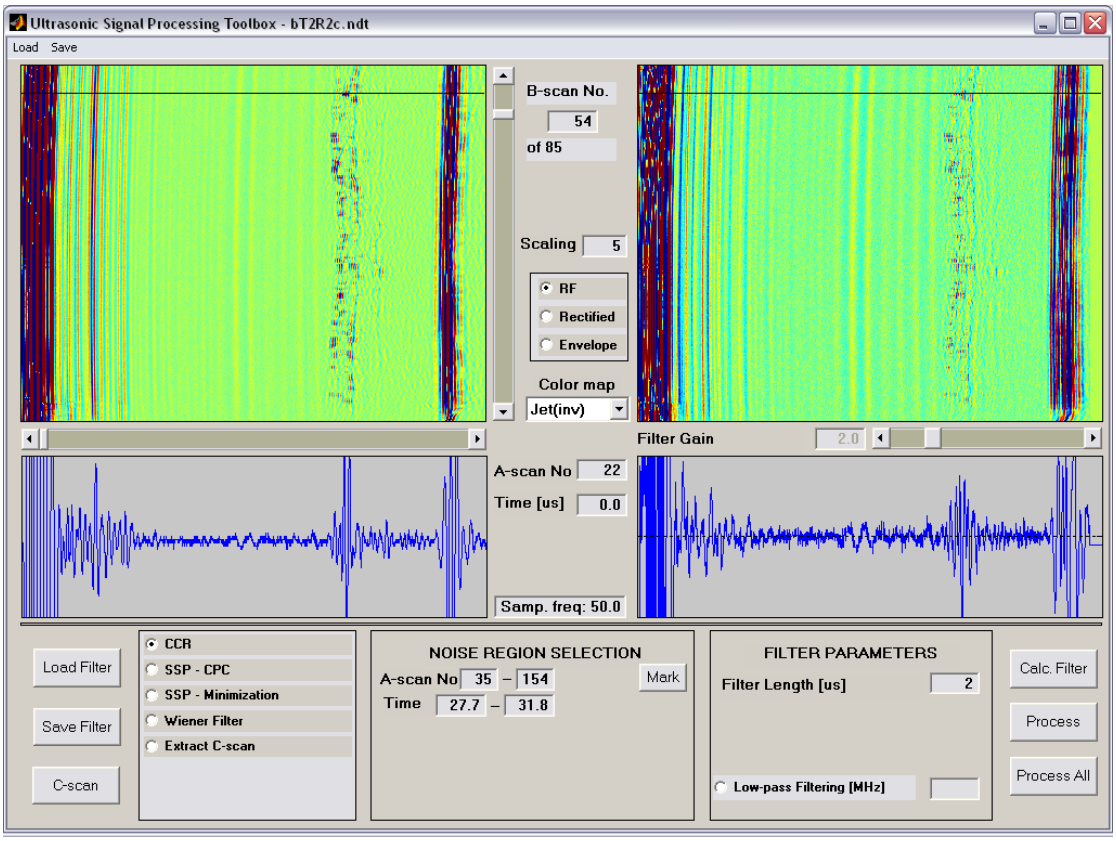

Fig. 4.2 An example of ultrasonic data, from the CAN1 block, processed using the filter shown in Figure 4.1. The A-scans correspond to the horizontal line running across the B-scans (A-scan number 22).

The A-scans presented below the B-scan windows are those corresponding to the horizontal black line running through the B-scans.

4.3 SSP Minimization

The Minimization method measures the correlation between the signals generated by the SSP filter bank by finding the minimum amplitude for each instance of time among them. If a

target is present the amplitude should be high in all frequency bands, while grain noise only should result in random amplitudes. Consequently, the result will be that grain noise is suppressed compared to target echoes. Figure 4.3 shows the result of Minimization method applied on ultrasonic data from the CAN1 block:

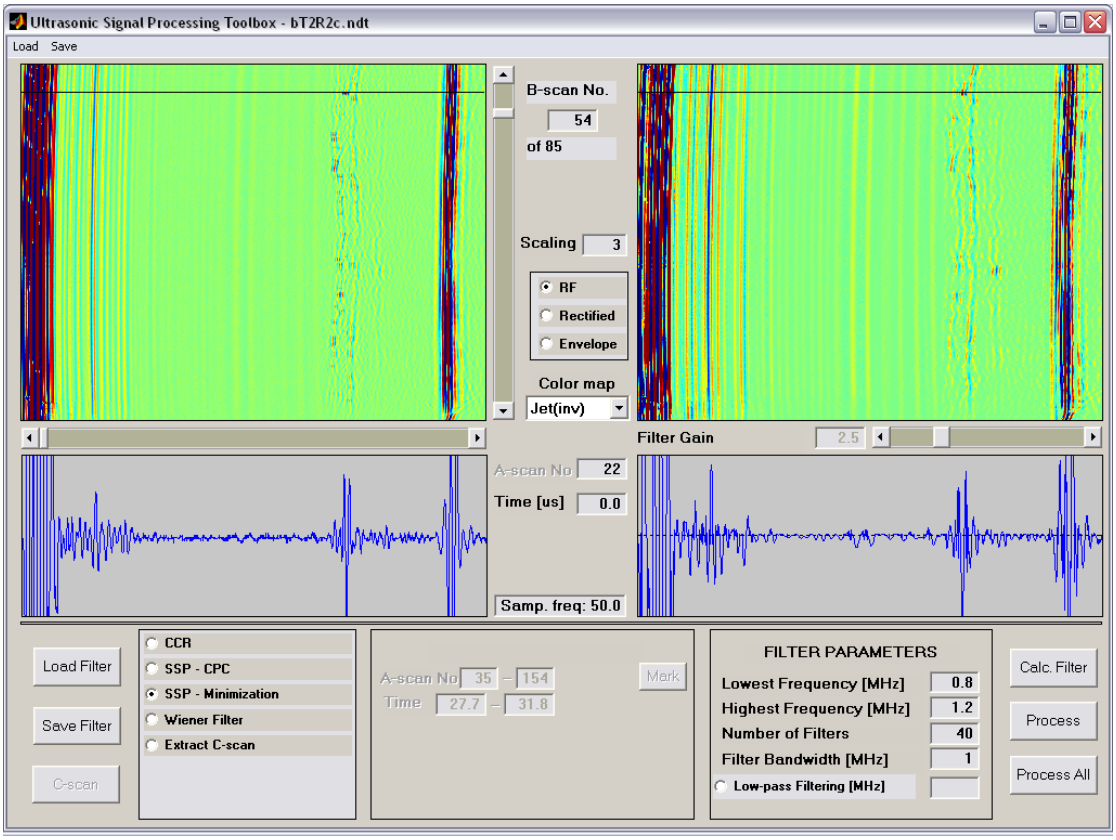

Fig. 4.3 An example of ultrasonic data from the CAN1 block being processed with the Minimization method. The A-scans correspond to the horizontal line running across the B-scans (A-scan number 22).

The figure presents the original and the processed B-scans and A-scans. As shown in the figure the processed B-scan has suppressed parts of the noisy welded area while the defects remain within the B-scan. This method does suppress parts of the noise and improve the signal to noise ratio, however it fails to totally remove the effects of the weld as parts of the weld behaves much like the artificial holes within the welded are. The choice of filter parameters is very important for the performance of the method. The more number of filters used the better will the result be, however increasing the number of filters also slows down the method significantly. Using too few filters results in poor noise regression but could also result in the loss of target echo as these echoes may be in the frequency band that is not covered by the filter. The same will occur if the target echo falls out of the frequency range

given by Lowest and Highest Frequency parameters. These possible failures, along with the original A-scan, are illustrated in Figure 4.4

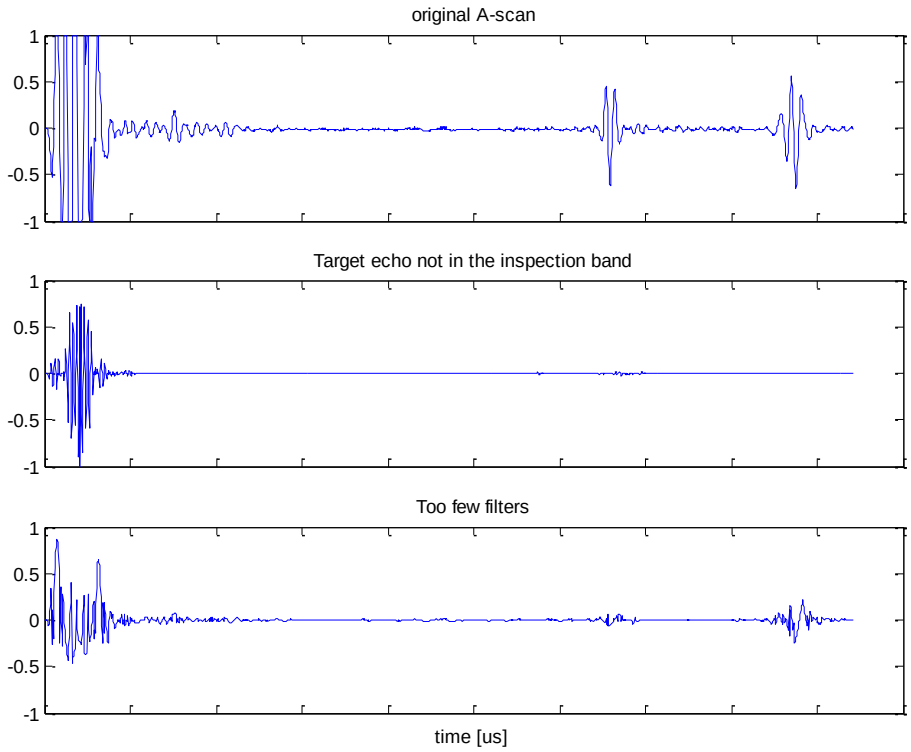

Fig. 4.4 An example of target echo elimination due to poor choice of filter parameter values.

The result of bad choice of parameters is observed in Figure 4.4. In the first case the filter is set to inspect frequencies in the range [5 to 6] MHz while the second failure is due to the use of only 2 filters.

4.4 SSP Consecutive Polarity Coincidence

The CPC is the second SSP-extraction method used in this toolbox. The extraction algorithm counts the number of split signals having equal polarity, in sequence. The longer these sequences are the better are the chances that they originate from a defect. Figure 4.5 shows the result of the CPC method applied to a B-scan.

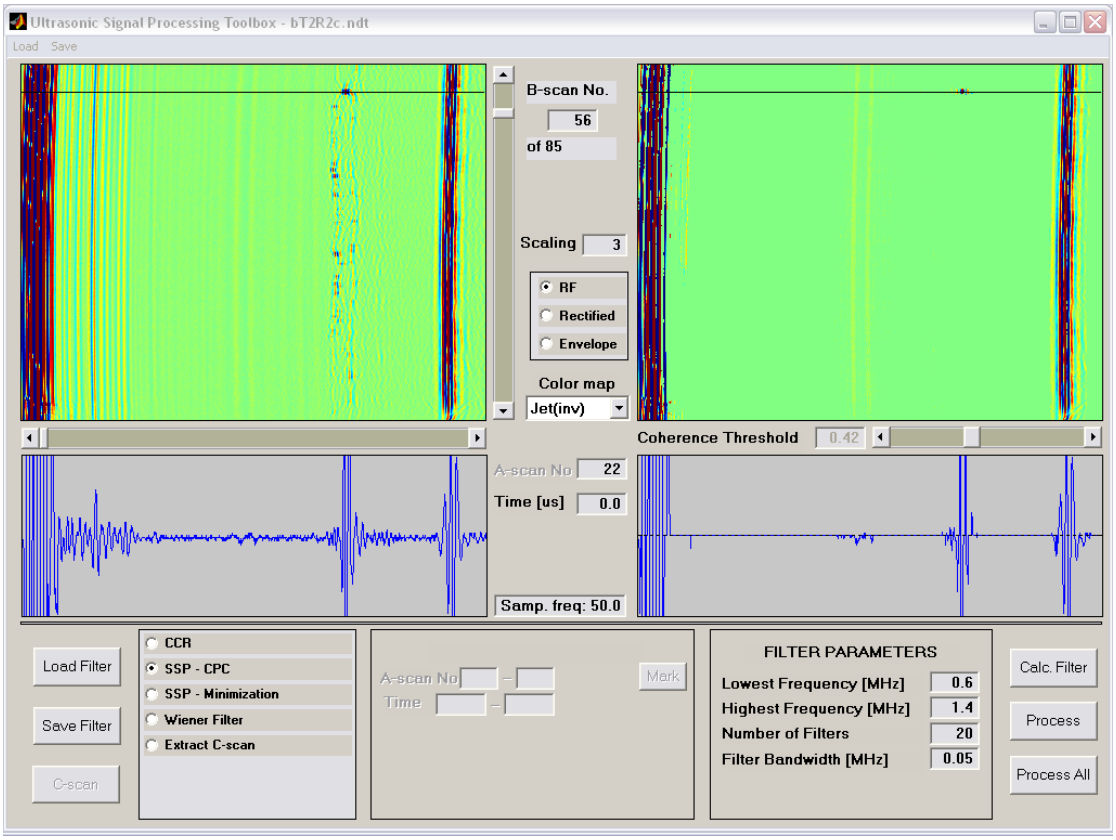

Fig. 4.5 An example of the CPC method applied on ultrasonic data from the CAN1 block. The A-scans correspond to the horizontal line running across the B-scans (A-scan number 22).

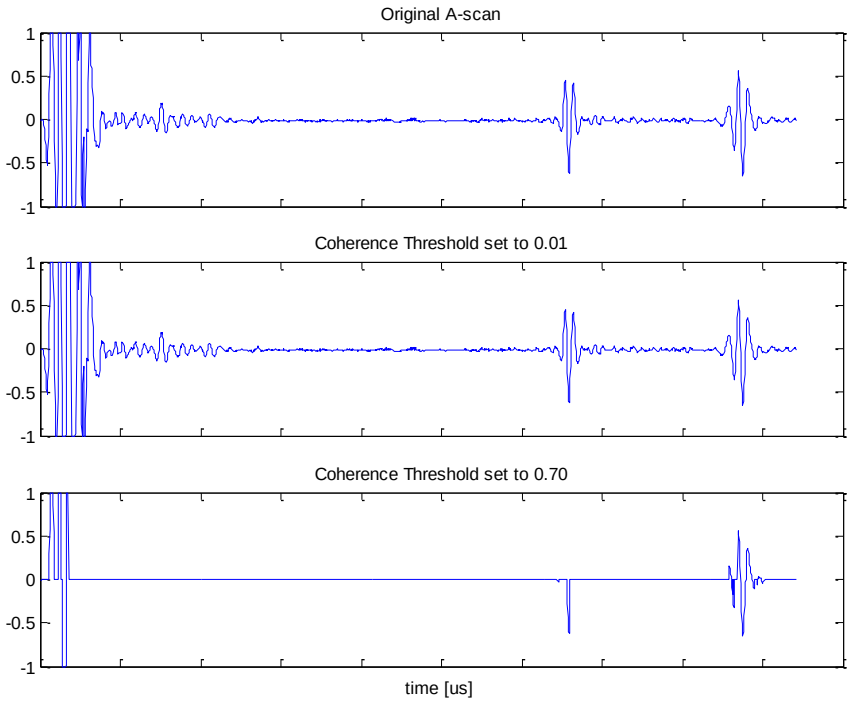

Fig. 4.6 An example of how Coherence Threshold effects the output of the filter. A low threshold value doesn't filtrate the scan at all while a high value can eliminate the target echo (here the Coherence Threshold of 0.71 resulted in such an elimination).

As shown in Figure 4.5 above, the method has removed the areas containing noise while signals originating from target remain in the output. As in the case for the Minimization method, a poor choice of parameters can result in eliminating the target echoes. The only additional parameter (as compared to the Minimization method) is the *Coherence Threshold*. An example of how different choices of this parameter can affect the result is shown in Figure 4.6.

4.5 Wiener deconvolution

The Wiener deconvolution method, as explained in section 2.9, is used to enhance the temporal resolution within the B-scans. This suggests that the location of the target echoes can be decided with a higher accuracy. Figure 4.4 shows the design of filter used for Wiener deconvolution.

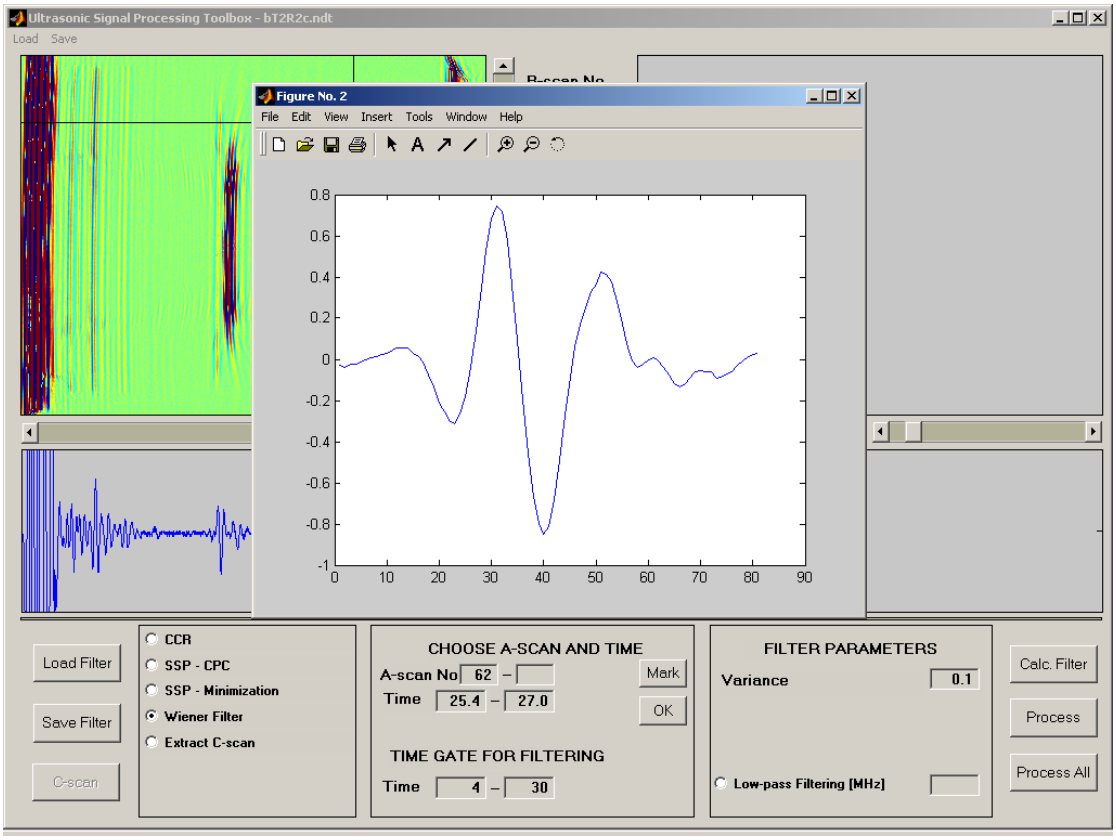

Fig. 4.5 An example of a filter used for the Wiener deconvolution process taken from the CAN1 block.

The filter used is an approximation of the inverse of the frequency response described in section 2.9. For more information on how to extract parts of an A-scan see the Manual in Appendix B. The result of the filtering process using the filter shown in Figure 4.5 is presented in Figure 4.6:

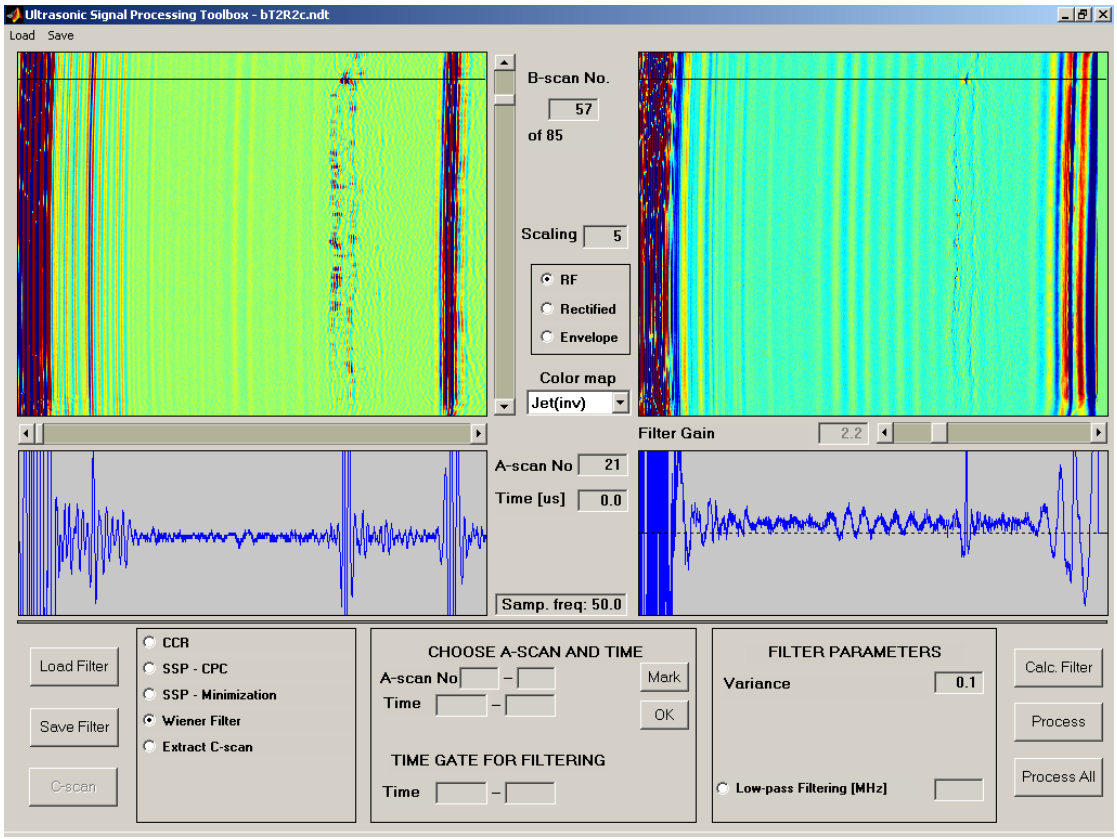

Fig. 4.6 An example of ultrasonic data being processed using the Wiener filter in Figure 4.5 and variance value of 0.1. The A-scans correspond to the horizontal line running across the B-scans (A-scan number 21).

Figure 4.6 shows the result of processing ultrasonic data from the CAN1 block using the Wiener filter shown in Figure 4.5. The higher temporal resolution is seen as sharper defect echoes.

5 Conclusion and Further Work

The results show that sonic inspection of the joints is a very useful method for detecting voids and irregularities in the sample. However, the previous chapter also shows that applying correct filters to enhance the signal to noise ratio without loss of critical data is difficult and needs much more study. The most valuable function of the toolbox, so far, is the visualisation of the weld and voids. This function together with the low pass filter designed to remove noise is very helpful in identifying risk areas in the sample.

Next step in developing the toolbox should be to study more samples in order to find better filter applications to enhance the picture and map the voids so that correct void size – and shape - can be extracted out of the data. Also, further developing the *Adaptive C-scan extraction* will help the operator to focus on crucial parts of the sample.

Another useful development should be to automatize the toolbox and add a self-learning mechanism to allow further improvement of the toolbox by evaluating many samples. It is also valuable to generate reports on samples which would make it possible to evaluate more samples with less operator supervision.

Perhaps the most difficult part is deciding what voids would be acceptable in the final canisters, this however is more a subject for a Material Science study.

Bibliography

[1] CLAB - Central interim storage facility for spent nuclear fuel, SKB, “Information material year 2000”, Available: Vi tar hand om det svenska radioaktiva avfallet (skb.se) [Accessed: September 2002].

[2] F. Gustafsson, L. Ljung and M. Millnert, *Signalbehandling*, Studentlitteratur AB, 2001.

[3] E. Pärt-Enander, A. Sjöberg, *Användarhandledning för MATLAB 6*, Uppsala: Avd. för teknisk databehandling, 2003.

[4] Mathworks, *Matlab 6.1 user guide*, Mathworks, 2003.

[5] D. E. Bray, R. K. Stanley, *Nondestructive evaluation: A tool in Design, Manufacturing, and Service*, CRC Press, 1997.

[6] R. Meddins, *Introduction to Digital Signal Processing*, Newnes, 2000.

[7] L. Ericsson, “Reduction of material noise in ultrasonic non-destructive evaluation using synthetic frequency diversity algorithm”, Signals and Systems, Uppsala University, Uppsala, Sweden, Tech. Report. 1994.

[8] T. Stepinski, L. Ericsson, “Signal Processing for Ultrasonic Testing Materials with Coarse Structure”, Signals and Systems, Uppsala University, Uppsala, Sweden, Tech. Report. 2000.

[9] L. Ericsson, T. Stepinski, “Algorithms for Suppressing Ultrasonic Backscattering from Material Structure – A Review”, Signals and Systems, Uppsala University, Uppsala, Sweden, Tech. Report. 2001-06-30.

[10] T. Stepinski, P. Wu, “Ultrasonic Technique for Imaging Welds in Copper”, Proceedings of the 16th IEEE Instrumentation and Measurement Technology Conference, Venice, Italy, 24-26 May 1999.

[11] M. H. Hayes, *Statistical Digital Signal Processing and Modelling*, John Wiley And Sons Ltd, 1996.

Appendix A

The Signals and Systems group at Uppsala University has gathered the ultrasonic data that has been processed and presented within this thesis. The test-object referred to throughout the report is shown in figure A.1:

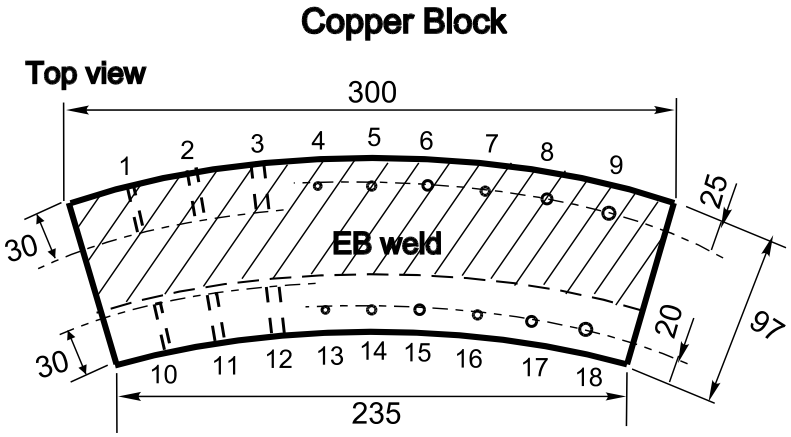

Hole No.	1	2	3	4	5	6	7	8	9
	10	11	12	13	14	15	16	17	18
Type	SDH			FBH			RBH		
Diameter	1.0	1.5	2.0	1.5	2.0	2.5	2.0	2.5	3.0

Fig. A.1 The cross section of the copper block.

The electronic beam weld is situated 60 mm below the upper surface. The holes within the weld zone are identical to those outside the weld in order to visualize the effect of the electronic beam weld on defects as well as to simplify the evaluation of the processing methods (since finding defects within the weld zone is the focus of the processing methods).